

Article

Tensile Fatigue Properties of Ordinary Plain Concrete and Reinforced Concrete under Flexural Loading

Huating Chen ^{1,*} , Zhenyu Sun ¹, Xianwei Zhang ² and Jinhong Fan ³

¹ Faculty of Architecture, Civil and Transportation Engineering, Beijing University of Technology, Beijing 100124, China; szszy990509@emails.bjut.edu.cn

² CCCC First Harbor Engineering Survey and Design Institute Co., Ltd., Tianjin 300222, China; zhangxianwei7@ccccltd.cn

³ Faculty of Materials and Manufacturing, Beijing University of Technology, Beijing 100124, China; fanjinhong@bjut.edu.cn

* Correspondence: chenhuating@bjut.edu.cn; Tel.: +86-133-0113-7705

Abstract: Many bridge structural components are subjected to repetitive vehicle load and temperature gradient action. The resulting cyclic tensile stresses within the structures could cause premature fatigue failure of concrete, dramatically impairing structural components' durability and sustainability. Although substantial knowledge of fatigue properties on low-strength pavement concrete and high-strength structural concrete has been obtained, research on the most widely used normal-grade ordinary concrete in bridge engineering is still ongoing. Therefore, a four-point bending fatigue test of 97 C50 concrete specimens under a constant amplitude sinusoidal wave was conducted in the laboratory, the flexural fatigue behavior of plain and reinforced concrete specimens was studied, and the cyclic deformation evolution of concrete under fatigue loading was obtained. The empirical fatigue $S-N$ equations of concrete with a failure probability p of 0.1~0.5 were derived through statistical analysis of the test results. The fatigue life of the tested specimens exhibited a two-parameter Weibull distribution. In addition to the maximum stress level S_{\max} , the stress ratio R is also a key factor affecting the flexural fatigue life of concrete N . The semi-logarithmic and logarithmic equations were almost identical at the tested stress levels, the latter predicting longer fatigue life for $S_{\max} < 0.70$. The restraining effect from steel reinforcement slightly lengthened the concrete's fatigue cracking initiation life. The insight into concrete flexural fatigue properties from this study not only contributes to a better understanding of structural concrete, but also provides a basis for the practical evaluation of concrete or composite bridge decks.

Keywords: flexural fatigue behavior; ordinary concrete; fatigue $S-N$ equations; fatigue strain; fatigue stress-strain curve; Weibull distribution; effect of reinforcement



Citation: Chen, H.; Sun, Z.; Zhang, X.; Fan, J. Tensile Fatigue Properties of Ordinary Plain Concrete and Reinforced Concrete under Flexural Loading. *Materials* **2023**, *16*, 6447. <https://doi.org/10.3390/ma16196447>

Academic Editor: Firas Al Mahmoud

Received: 28 August 2023
Revised: 20 September 2023
Accepted: 21 September 2023
Published: 28 September 2023



Copyright: © 2023 by the authors. Licensee MDPI, Basel, Switzerland. This article is an open access article distributed under the terms and conditions of the Creative Commons Attribution (CC BY) license (<https://creativecommons.org/licenses/by/4.0/>).

1. Introduction

With the increasing vehicle axle loads, concrete bridge decks and other bridge components are prone to fatigue cracking under repeated wheel loading [1]. Once the concrete cracks, the long-term durability of concrete and internal steel reinforcement will be significantly affected, and the service life of the bridge deck will be reduced. Afterward, the elevated tensile stress amplitude induced in the reinforcement and the compressive stress in concrete may lead to performance deterioration or even premature fatigue failure of the bridge deck at loads far lower than its static bearing capacity. As concrete failure is closely related to cracks caused by tension [2], flexural tensile fatigue properties of concrete are fundamental to understanding and evaluating the fatigue cracking behavior of such bridge components, particularly when strengthening existing concrete bridges is necessary.

The flexural tensile fatigue properties of concrete are primarily obtained through constant amplitude fatigue tests of small-scale beam specimens loaded in four-point or three-point bending. Scholars have conducted numerous experimental studies on the

flexural tensile fatigue of concrete since the 1970s [3], and the effects of many relevant parameters, such as the stress level, stress ratio, failure probability, and loading frequency, on fatigue life have been investigated [4–6]. After statistical and regression analysis of fatigue life data, various forms, semi-logarithm or logarithm, of fatigue life equations have been obtained [5]. For example, concrete bending fatigue *S-N* equations under a fixed stress ratio were proposed in the literature [7,8], and probabilistic fatigue *S-N* equations considering the influence of the stress ratio and failure probability were proposed in [9,10]. In the recent two decades, the primary focus of research on flexural tensile fatigue properties has shifted towards the effects of fiber reinforcement [11,12], mineral admixtures [13], lightweight aggregates [14,15], and recycled aggregates [16–18]. Existing works are mainly conducted on low-strength or high-strength ordinary concrete traditionally and on innovative composite concrete recently. Nevertheless, the research on normal-grade ordinary concrete commonly used in bridge engineering, say, C40–C60, is limited.

While fatigue life is still the primary focus in concrete fatigue research, more and more researchers are paying attention to the accumulation and evolution of fatigue damage during the entire process of fatigue loading [19]. Different physical parameters, such as maximum strain [20], residual strain [21,22], and deformation modulus [23], have been correlated with fatigue damage variables. Experimental investigations that report concrete strain, in addition to applied stress, could provide a fundamental database to study fatigue damage variables and their evolution.

Although reinforced concrete members are often used in actual engineering structures, plain concrete specimens are usually employed in bending fatigue tests. The effect of steel reinforcement on concrete fatigue cracking has yet to be fully explored [24]. Therefore, based on C50 ordinary concrete, which is most widely used in bridge engineering in China, this paper directly compares the difference in fatigue cracking performance between plain concrete and reinforced concrete specimens through four-point bending fatigue tests. The distribution of concrete fatigue cracking life is studied through regression analysis of test data, and the probabilistic fatigue equation of concrete in flexural tension considering the stress ratio and failure probability is obtained. In addition, the longitudinal concrete strain will be recorded during the fatigue test to provide essential data for constructing a concrete fatigue damage constitutive model. With continuously recorded strain data, the novelty of this study lies in obtaining the fatigue characteristics of C50 plain and reinforced concrete specimens through direct comparison.

2. Materials and Methods

2.1. Materials and Mix Design

The ordinary concrete selected for this study was commercial C50 concrete, thanks to its wide application in bridge engineering. The mix ratio was cement/sand/stone/water = 1:1.93:3.02:0.46. Among these, the cement was ordinary 425 Portland cement produced by a local plant, the sand was medium natural sand with a fineness modulus of 2.4, and the coarse aggregate was rubble and cobble gravel with a maximum particle size of 25 mm. The target slump was 180 ± 20 mm. A high-performance water-reducing agent STD-PCS of 1.99% was added for improved workability. The water-reducing agent STD-PCS was a polycarboxylic acid-type superplasticizer manufactured by a local company (Tianjin Steady Industrial Development Co., Ltd., Tianjin, China). The workability of fresh mixtures was evaluated with the standard slump cone with dimensions of a 100 mm diameter on the top, a 200 mm diameter on the bottom, and 300 mm high. More information about the concrete mix is given in Table 1.

The steel reinforcement under consideration was the commonly used grade HRB400. The standard values of the steel's yield strength, tensile strength, elastic modulus, and elongation percentage are 400 MPa, 540 MPa, 200 GPa, and 16%, respectively.

Table 1. Details of concrete mix.

| Materials | Cement | Fine Aggregate | Coarse Aggregate | Water | Admixture | Mineral Powder | Fly Ash |
|-----------------------------|---------|----------------|---------------------|-------|-----------|----------------|---------|
| Properties | PO 42.5 | Medium sand | Crushed, 5~25 mm | – | STD-PCS | S95 | IIF |
| Amount (kg/m ³) | 347 | 670 | 1048 | 160 | 9.2 | 69 | 46 |
| Mix proportion | 1 | 1.93 | 3.02 | 0.46 | 0.03 | 0.20 | 0.13 |

2.2. Specimen Preparation

Standard flexural strength specimens with dimensions of 150 mm × 150 mm × 550 mm, as shown in Figure 1 and specified in the Chinese Standard GB/T 50081-2019 for the test method of mechanical properties on ordinary concrete [25], were adopted. Altogether, 132 specimens were prepared in two series, 66 specimens for each, namely a PC series and RC series. All PC specimens were made from plain concrete, while the RC series consisted of 48 reinforced concrete beams supplemented by 18 plain concrete beams. Six companion 150 mm × 150 mm × 150 mm concrete cubes were obtained for each beam specimen series to verify the concrete grade through the compressive strength test.

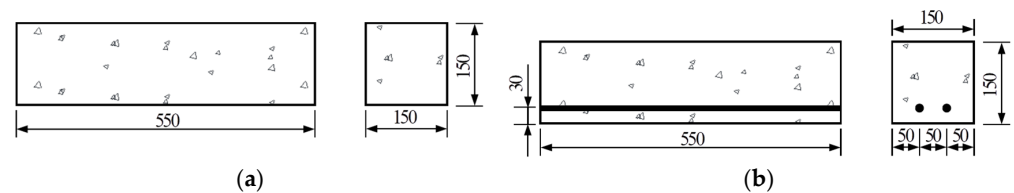


Figure 1. Beam specimens (dimensions in mm): (a) plain concrete specimens in PC and RC series; (b) reinforced concrete specimens in RC series.

The reinforced concrete specimens were identical to their plain concrete counterparts except for reinforcement. A reinforcement ratio of 1%, which is typical in concrete bridge decks, was provided in the reinforced concrete specimens. Two full-length grade HRB400 Φ 12 mm reinforcing bars were placed in the bottom part of each specimen, with a concrete cover of 30 mm. A schematic diagram of the reinforced concrete specimens is shown in Figure 1b.

All specimens were produced with a wooden formwork. After concrete pouring, the specimens were covered with a polyethylene sheet and cured for 28 days under standard curing conditions (at a temperature of 22 °C and a relative humidity of 95%). After 28 days of standard curing, the specimens were stored in the Mechanics Laboratory near the testing machine. No special treatment was provided. Roughly, they were exposed to a room temperature of 17~27 °C and relative humidity of 30~80%. At the time of testing, the age of the specimens was 35~60 days. Figure 2 shows a photo of the specimen preparation during the concrete pouring.



Figure 2. Specimen preparation during concrete pouring.

2.3. Testing Set-Up and Loading Matrix

All beam specimens were tested under four-point bending conditions, as shown schematically in Figure 3a. A standard static flexural test was conducted before the fatigue test to obtain the flexural strength. A total of 9 specimens from the PC series and 24 specimens (including 18 plain concrete beams and 6 additional reinforced concrete beams) from the RC series were tested by a static test machine, shown in Figure 3b. For the reinforced concrete specimens, the flexural strength was determined when a macroscopic concrete crack appeared at the side surfaces of the tested beam.

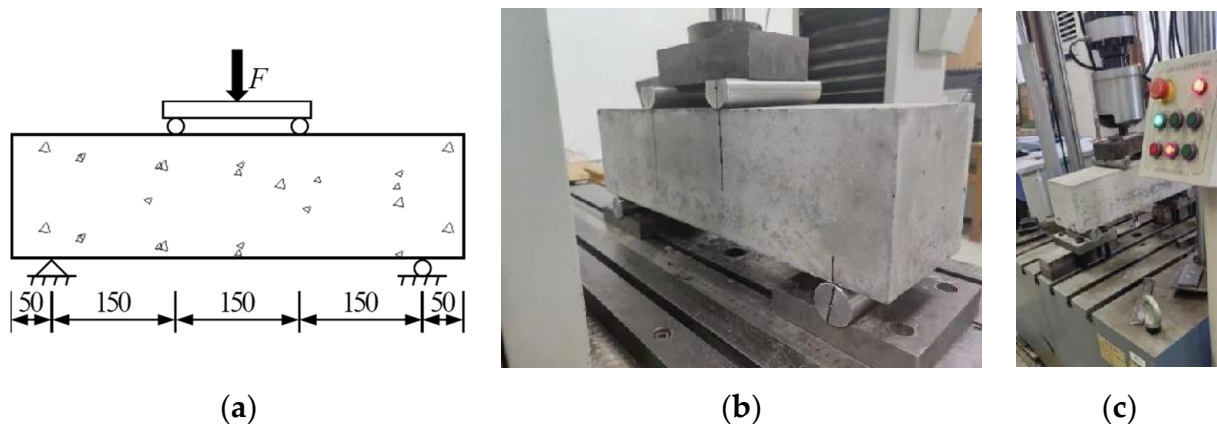


Figure 3. Four-point bending test: (a) scheme of test set-up (dimensions in mm); (b) photo of static test set-up; (c) photo of fatigue test set-up.

The fatigue test was conducted with a QBS-50A electro-hydraulic servo-controlled universal testing machine in the Engineering Mechanics Laboratory at the Beijing University of Technology. The testing machine, manufactured by Changchun Qianbang Testing Equipment Co., Ltd. (Changchun, China), has a maximum load capacity of 50 kN and a loading frequency of 0.1~10 Hz, as shown in Figure 3c.

A fatigue loading matrix with combinations of the maximum and minimum stress levels was designed. Stress levels are defined as the fatigue stresses divided by the static strength. The stress ratio R is the ratio between the minimum stress level S_{\min} and the maximum stress level S_{\max} . S_{\max} in the range of 0.65~0.90, and S_{\min} of 0.10, 0.25, and 0.4 were considered in the test program. The fatigue test matrix for the PC series (plain concrete specimens) and RC series (reinforced concrete specimens) is shown in Table 2. A constant amplitude sinusoidal wave was applied to maintain the desired stress levels. Due to the limitation of the testing machine, 15 specimens with a maximum stress level of 0.9 were tested with a slower frequency of 0.1 Hz. All other specimens were tested with a frequency of 5 Hz. Specimens were positioned correctly on the fatigue testing machine, and the parameters were adjusted to obtain the desired fatigue load waveform and frequency, as shown in Figure 3c.

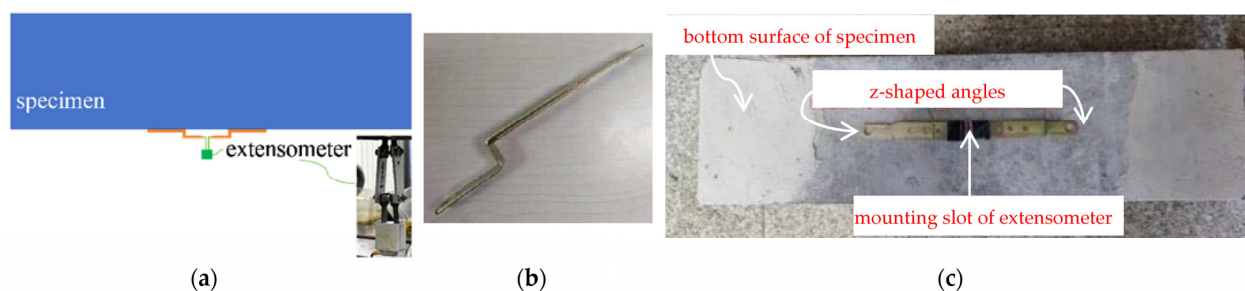
Fatigue failure is defined when a plain concrete specimen breaks or a macroscopic concrete crack appears at the side surfaces of a reinforced concrete specimen. The fatigue test was terminated at the time of failure or after a predetermined number of cycles. A specimen undergoing no signs of failure after 1 million loading cycles was terminated in the fatigue test for plain concrete specimens and was termed run-out. For the reinforced concrete specimens, fatigue loading usually continued after the first sign of concrete cracking until far surpassing the observed fatigue life of the plain concrete counterparts tested under similar stress levels. The predetermined number of cycles for the fatigue test termination of the RC series was between 10,000 and 80,000, depending on the tested stress levels.

Table 2. Fatigue test matrix of PC series (plain concrete specimens) and RC series (reinforced concrete specimens).

| Series | Set No. | Maximum Stress Level S_{max} | Minimum Stress Level S_{min} | Stress Ratio R | Number of Specimens | Test Frequency (Hz) |
|--------|---------|-----------------------------------|-----------------------------------|---------------------|---------------------|---------------------|
| PC | 1 | 0.90 | 0.10 | 0.110 | 5 | 0.1 |
| | 2 | 0.90 | 0.25 | 0.280 | 5 | 0.1 |
| | 3 | 0.90 | 0.40 | 0.440 | 5 | 0.1 |
| | 4 | 0.80 | 0.10 | 0.125 | 12 | 5 |
| | 5 | 0.75 | 0.10 | 0.133 | 13 | 5 |
| | 6 | 0.75 | 0.25 | 0.333 | 12 | 5 |
| | 7 | 0.65 | 0.10 | 0.154 | 3 | 5 |
| RC | 1 | 0.85 | 0.10 | 0.117 | 7 | 5 |
| | 2 | 0.85 | 0.25 | 0.294 | 7 | 5 |
| | 3 | 0.80 | 0.10 | 0.125 | 7 | 5 |
| | 4 | 0.80 | 0.25 | 0.313 | 7 | 5 |
| | 5 | 0.75 | 0.10 | 0.133 | 7 | 5 |
| | 6 | 0.75 | 0.25 | 0.333 | 7 | 5 |

2.4. Measurement and Instrumentation

The fatigue testing machine automatically recorded load, displacement, and the number of cycles of the actuator, and a real-time stress-versus-time curve was displayed to facilitate test monitoring. For continuous measuring of the strain during the fatigue test, an extensometer was used to determine the average strain at the bottom surface of the specimen over the pure bending region, i.e., the middle third of the span. A YYJ-(−2)-5/6 extensometer, manufactured by NCS Testing Technology Co., Ltd. (Beijing, China), has a default gauge length of 6 mm, a measurement range between −2 mm and 5 mm, and a measuring sensitivity of 0.001 mm. Rigid Z-shaped angles were glued to the bottom surfaces of test specimens to ensure cracks occurred within the gauge length. The gauge length was thus extended to 90 mm for plain concrete specimens and 146 mm for reinforced concrete specimens, respectively. Figure 4 shows the arrangement of Z-shaped angles.

**Figure 4.** Devices to extend the range of extensometer measurements: (a) scheme of strain measurement; (b) Z-shaped angle; (c) arrangement of angles for extensometer installation.

2.5. Fatigue Life Distribution

The observed fatigue life of concrete specimens is a random variable with great discreteness. When the fatigue life data were arranged in ascending order, the failure probability p of a particular specimen could be estimated by the average rank as in the following expression [14]:

$$p = \frac{i}{k + 1} \quad (1)$$

where i denotes the failure order, and k is the total number of specimens tested at a particular stress level.

Concrete fatigue life is generally assumed to conform to the two-parameter Weibull distribution [4,9]. Accordingly, the failure probability p satisfies Equation (2). Equation (3)

can be derived to test whether a group of experimental results follows the two-parameter Weibull distribution. Suppose the regression analysis of the experimental data can show a good statistical linear relationship between $\ln \ln(1/(1-p))$ and $\ln N$; that is, the coefficient of determination R^2 is relatively high. In that case, this assumption is valid, and vice versa.

$$p = F(N) = 1 - e^{-N^m/t_0} \quad (N \geq 1 \text{ and } t_0 > 0) \quad (2)$$

$$\ln \ln(1/(1-p)) = m \ln N - \ln t_0 \quad (3)$$

where m is the shape parameter, and the scale parameter can be expressed as $t_0^{1/m}$.

Recall that the experiment program includes specimens tested with combinations of the maximum and minimum stress levels, as described in Section 2.3 and Table 2. While the maximum stress level S_{\max} is of primary concern, it is desirable to consider the effect of the stress ratio R on the probabilistic distribution of fatigue life. According to the literature [9], using equivalent fatigue life, that is, $\bar{N} = N^{1-R}$, all experimental data with the same S_{\max} can be combined for statistical analysis. The equations for the Weibull distribution test can be rewritten as follows:

$$p = F(\bar{N}) = 1 - e^{-\bar{N}^m/t_0} \quad (\bar{N} \geq 1 \text{ and } t_0 > 0) \quad (4)$$

$$\ln \ln(1/(1-p)) = m \ln \bar{N} - \ln t_0 \quad (5)$$

2.6. S-N Curves

Various fatigue S-N equations have been proposed. The maximum stress level S_{\max} has traditionally been written as S for conciseness. While the dependent variable fatigue life N is always expressed in logarithm, the independent variable can either be S or the logarithm of S . Some S-N curves apply to fatigue tests conducted at a fixed minimum stress level, usually close to 0, and others can consider the effect of the stress ratio R .

The semi-logarithmic and logarithmic fatigue equations for specimens fatigue-tested with a fixed minimum stress level are expressed as follows:

$$S = a - b \lg N \quad (6)$$

$$\lg S = A - B \lg N \quad (7)$$

where intercept a or A is the basic strength corresponding to $N = 1$, and slope b or B is called the fatigue strength exponent.

The semi-logarithmic and logarithmic fatigue equations, when considering the stress ratio R , can be expressed as follows:

$$S = a - b(1-R) \lg N = a - b \lg \bar{N} \quad (8)$$

$$\lg S = A - B(1-R) \lg N = A - B \lg \bar{N} \quad (9)$$

where the constants a , b , A , and B have the same physical meaning as those in Equations (6) and (7), except equivalent fatigue life \bar{N} is considered.

A direct quantitative relationship between fatigue life and failure probability could be established for reliability analysis applications. Probabilistic fatigue equations are obtained by substituting the fatigue life of various failure probabilities into Equations (6)–(9), Equations (6) and (7) for constant S_{\min} of 0.10, and Equations (8) and (9) when considering the stress ratio. If the fatigue life or equivalent fatigue life correlates with two-parameter Weibull distribution, the fatigue life N , or equivalent fatigue life \bar{N} when considering the

stress ratio, corresponding to a given failure probability p , can be calculated by Equation (10) by rewriting Equations (2) and (4).

$$N \text{ or } \bar{N} = [\ln(1/(1-p)) \times t_0]^{1/m} \quad (10)$$

3. Results and Discussion

Fatigue test results were obtained from 55 plain concrete specimens (PC series) and 42 reinforced concrete specimens (RC series). The maximum and minimum fatigue stresses were determined from the preset stress levels (Table 2) and the average flexural strength of each series. The compressive strength of concrete cubes was utilized to verify the strength grade of the concrete mixes.

3.1. Test Results

3.1.1. Material Characterization

The compressive strength was obtained from standard tests on six cubic specimens for each series. The test results, along with the statistical values, are shown in Table 3. The 28-day average compressive strengths of the PC and RC series were 53.9 MPa and 51.1 MPa, respectively. Both concrete batches met the strength requirement of commercial grade 50 concrete, while the RC series had a 5% lower average strength than the PC series. However, the material dispersion of the RC series was significantly smaller than that of the PC series.

Table 3. Compressive strength of concrete mixes.

| Series | Measured Compressive Strength (MPa) | | | | | | Statistical Characteristics | | |
|--------|-------------------------------------|--------|--------|--------|--------|--------|-----------------------------|--------------------------|--------------------------|
| | Cube 1 | Cube 2 | Cube 3 | Cube 4 | Cube 5 | Cube 6 | Mean Value (MPa) | Standard Deviation (MPa) | Coefficient of Variation |
| PC | 51.0 | 47.4 | 61.2 | 41.6 | 61.6 | 60.8 | 53.9 | 7.77 | 0.14 |
| RC | 51.2 | 52.1 | 51.4 | 50.2 | 51.5 | 50.2 | 51.1 | 0.76 | 0.015 |

Concrete flexural strength was obtained from standard four-point bending tests on 9 PC series beam specimens and 24 RC series specimens. The six beams in Sets 7 and 8 of the RC series were specimens with reinforcement. While all plain concrete specimens fractured in the middle third region, the reinforced concrete specimens did not fail due to the strength of reinforcement. Therefore, the flexural strength of the concrete in the reinforced concrete specimens was determined when macroscopic cracks appeared on the side surfaces of the beams.

The measured static flexural strengths of the two batches of concrete, along with the statistical values, are shown in Table 4. The average flexural strength of the RC series was 9% lower than the PC series, which is consistent with the relative values of their compressive strength. The coefficients of variation between the two series are almost identical. Statistically, reinforced concrete specimens show slightly smaller flexural strength than plain concrete specimens.

Table 4. Static flexural strength of concrete mixes.

| Series | Measured Flexural Strength (MPa) | | | | | | | | Statistical Characteristics | | |
|--------|----------------------------------|-------|-------|-------|-------|-------|-------|-------|-----------------------------|--------------------------|--------------------------|
| | Set 1 | Set 2 | Set 3 | Set 4 | Set 5 | Set 6 | Set 7 | Set 8 | Mean Value (MPa) | Standard Deviation (MPa) | Coefficient of Variation |
| PC | 6.6 | 5.3 | 6.0 | – | – | – | – | – | 5.6 | 0.55 | 0.10 |
| | 5.9 | 4.8 | 5.4 | – | – | – | – | – | | | |
| | 6.1 | 5.2 | 5.4 | – | – | – | – | – | | | |
| RC | 5.1 | 5.3 | 5.1 | 4.3 | 4.6 | 4.7 | 5.6 | 4.7 | 5.1 | 0.44 | 0.09 |
| | 5.2 | 3.8 | 4.5 | 4.8 | 4.2 | 4.5 | 5.6 | 5.3 | | | |
| | 4.5 | 4.7 | 4.9 | 4.7 | 3.8 | 4.8 | 5.5 | 5.4 | | | |

3.1.2. Failure Mode

Towards the end of the fatigue test, a vertical crack was observed to develop in the middle region in most plain concrete specimens, followed by a sudden fracture. The location of the fracture surface was random. However, all beams failed in the middle third pure bending region, and the fracture surface was generally planar. Most of the coarse aggregates were fractured, and a few pullouts of coarse aggregates along the interface between the coarse aggregates and cement mortar made the fracture surface zigzag. A typical fatigue failure of the plain concrete specimen is presented in Figure 5.

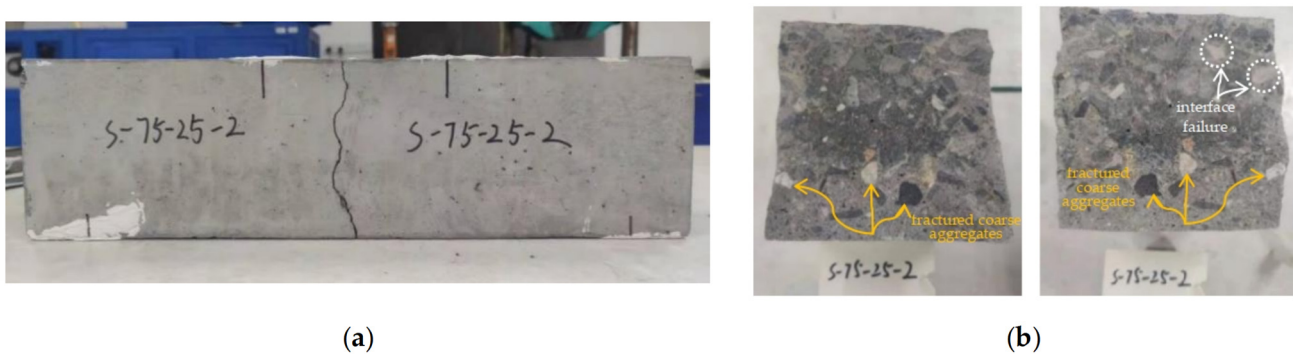


Figure 5. Typical fatigue failure of plain concrete specimens (PC series): (a) elevation view; (b) cross-section view.

For reinforced concrete specimens under fatigue loading, small cracks also occurred initially on the bottom surface within the pure bending region. After these cracks became macroscopic, they appeared on the side surfaces of the concrete specimen and slowly extended upward with the application of cyclic loading. At the same time, concrete cracks continued to develop at other locations of the pure bending region and gradually merged. Since there was tensile reinforcement, the specimen stiffness did not change apparently after concrete cracking, and it did not break abruptly. As the fatigue cracking life of concrete was the primary interest in this work, the fatigue test was stopped after visible cracks appeared on the side surfaces of specimens. A typical concrete fatigue failure of the reinforced concrete specimen is shown in Figure 6.



Figure 6. Typical fatigue failure of reinforced concrete specimens (RC series): (a) bottom surface; (b) side surface.

3.1.3. Fatigue Life

Fatigue life is the number of cycles a specimen can sustain before failure. The fatigue life of plain concrete specimens is summarized in Table 5. The specimen number is designated as S-a-b-x, where S means the tests are under stress control, a stands for the maximum stress level, b represents the minimum stress level, and x is the order of testing within the test set.

Table 5. Fatigue life test results of plain concrete specimens (PC series).

| Set No. | Set Designation | S_{max} | S_{min} | Specimen Designation | Fatigue Life N (Cycle) | Specimen Failure Order | Fatigue Life N (Cycle) | Failure Probability p |
|---------|-----------------|-----------|-----------|----------------------|--------------------------|------------------------|--------------------------|-------------------------|
| 1 | S-90-1 | 0.90 | 0.10 | S-90-1-1 | 12 | 1 | 3 | 0.17 |
| | | | | S-90-1-2 | 9 | 2 | 8 | 0.33 |
| | | | | S-90-1-3 | 9 | 3 | 9 | 0.50 |
| | | | | S-90-1-4 | 3 | 4 | 9 | 0.67 |
| | | | | S-90-1-5 | 8 | 5 | 12 | 0.83 |
| 2 | S-90-25 | 0.90 | 0.25 | S-90-25-1 | 415 | 1 | 110 | 0.17 |
| | | | | S-90-25-2 | 216 | 2 | 196 | 0.33 |
| | | | | S-90-25-3 | 110 | 3 | 216 | 0.50 |
| | | | | S-90-25-4 | 196 | 4 | 234 | 0.67 |
| | | | | S-90-25-5 | 234 | 5 | 415 | 0.83 |
| 3 | S-90-4 | 0.90 | 0.40 | S-90-4-1 | 1347 | 1 | 136 | 0.17 |
| | | | | S-90-4-2 | 136 | 2 | 370 | 0.33 |
| | | | | S-90-4-3 | 934 | 3 | 620 | 0.50 |
| | | | | S-90-4-4 | 620 | 4 | 934 | 0.67 |
| | | | | S-90-4-5 | 370 | 5 | 1347 | 0.83 |
| 4 | S-80-1 | 0.80 | 0.10 | S-80-1-1 | 3872 | 1 | 96 | 0.08 |
| | | | | S-80-1-2 | 96 | 2 | 261 | 0.17 |
| | | | | S-80-1-3 | 496 | 3 | 496 | 0.25 |
| | | | | S-80-1-4 | 6115 | 4 | 618 | 0.33 |
| | | | | S-80-1-5 | 1391 | 5 | 1036 | 0.42 |
| | | | | S-80-1-6 | 261 | 6 | 1391 | 0.50 |
| | | | | S-80-1-7 | 6358 | 7 | 3872 | 0.58 |
| | | | | S-80-1-8 | 61,960 ^a | 8 | 6115 | 0.67 |
| | | | | S-80-1-9 | 1036 | 9 | 6358 | 0.75 |
| | | | | S-80-1-10 | 618 | 10 | 6383 | 0.83 |
| | | | | S-80-1-11 | 8930 | 11 | 8930 | 0.92 |
| | | | | S-80-1-12 | 6383 | 12 | 61,960 ^a | – |
| 5 | S-75-1 | 0.75 | 0.10 | S-75-1-1 | 1658 | 1 | 63 | 0.08 |
| | | | | S-75-1-2 | 32,835 | 2 | 304 | 0.15 |
| | | | | S-75-1-3 | 14,444 | 3 | 380 | 0.23 |
| | | | | S-75-1-4 | 7574 | 4 | 528 | 0.31 |
| | | | | S-75-1-5 | 304 | 5 | 1658 | 0.38 |
| | | | | S-75-1-6 | 380 | 6 | 7574 | 0.46 |
| | | | | S-75-1-7 | 528 | 7 | 11,328 | 0.54 |
| | | | | S-75-1-8 | 63 | 8 | 14,048 | 0.62 |
| | | | | S-75-1-9 | 14,048 | 9 | 14,444 | 0.69 |
| | | | | S-75-1-10 | 224,931 ^a | 10 | 19,585 | 0.77 |
| | | | | S-75-1-11 | 11,328 | 11 | 32,835 | 0.85 |
| | | | | S-75-1-12 | 49,629 | 12 | 49,629 | 0.92 |
| | | | | S-75-1-13 | 19,585 | 13 | 224,931 ^a | – |
| 6 | S-75-25 | 0.75 | 0.25 | S-75-25-1 | 54,815 | 1 | 2518 | 0.08 |
| | | | | S-75-25-2 | 2518 | 2 | 5321 | 0.17 |
| | | | | S-75-25-3 | 365,759 ^a | 3 | 7308 | 0.25 |
| | | | | S-75-25-4 | 34,187 | 4 | 14,209 | 0.33 |
| | | | | S-75-25-5 | 5321 | 5 | 21,097 | 0.42 |
| | | | | S-75-25-6 | 7308 | 6 | 26,049 | 0.50 |
| | | | | S-75-25-7 | 68,135 | 7 | 32,646 | 0.58 |
| | | | | S-75-25-8 | 32,646 | 8 | 34,187 | 0.67 |
| | | | | S-75-25-9 | 26,049 | 9 | 39,379 | 0.75 |
| | | | | S-75-25-10 | 39,379 | 10 | 54,815 | 0.83 |
| | | | | S-75-25-11 | 14,209 | 11 | 68,135 | 0.92 |
| | | | | S-75-25-12 | 21,097 | 12 | 365,759 ^a | – |
| 7 | S-65-1 | 0.65 | 0.10 | S-65-1-1 | 1,000,000 [*] | 1 | 1,000,000 [*] | – |
| | | | | S-65-1-2 | 1,000,000 [*] | 2 | 1,000,000 [*] | – |
| | | | | S-65-1-3 | 1,000,000 [*] | 3 | 1,000,000 [*] | – |

^a Rejected as an outlier by Chauvenet's criterion, not included in further analysis. * Treated as run-out specimens, not included in further analysis.

Even in carefully controlled tests, it is observed in Table 5 that a significant difference in the fatigue life of several orders of magnitude existed for specimens within the same test set. The fatigue life results between different test sets are also remarkably different. Generally,

the fatigue life increased as the maximum stress level decreased when the minimum stress was kept constant or as the minimum stress level increased under the same maximum stress. Both the maximum and minimum stress levels affected the concrete's fatigue life.

Similarly, the reinforced concrete specimen is designated with an additional "J", as J-S-a-b-x, where all other parameters have the same meaning as in the PC series. Table 6 presents the fatigue cracking life data of the RC series in ascending order.

Table 6. Fatigue cracking life test results of reinforced concrete specimens (RC series).

| Set Designation | J-S-85-1 | J-S-85-25 | J-S-80-1 | J-S-80-25 | J-S-75-1 | J-S-75-25 |
|--|--------------------|---------------------|--------------------|-----------------------|----------------------|---------------------------------|
| S_{max} | 0.85 | 0.85 | 0.80 | 0.80 | 0.75 | 0.75 |
| S_{min} | 0.10 | 0.25 | 0.10 | 0.25 | 0.10 | 0.25 |
| Specimen designation Fatigue cracking life N (cycle) | J-S-85-1-2 228 | J-S-85-25-2 1765 | J-S-80-1-1 3782 | J-S-80-25-4 4870 | J-S-75-1-1 13,213 | J-S-75-25-1 598 ^a |
| | J-S-85-1-3 516 | J-S-85-25-5 1976 | J-S-80-1-6 4028 | J-S-80-25-7 6780 | J-S-75-1-3 14,274 | J-S-75-25-2 32,730 |
| | J-S-85-1-5 586 | J-S-85-25-4 2249 | J-S-80-1-3 4517 | J-S-80-25-6 8976 | J-S-75-1-4 14,680 | J-S-75-25-3 35,214 |
| | J-S-85-1-6 611 | J-S-85-25-1 2331 | J-S-80-1-2 5087 | J-S-80-25-5 9307 | J-S-75-1-2 16,030 | J-S-75-25-5 38,683 |
| | J-S-85-1-4 634 | J-S-85-25-3 2544 | J-S-80-1-4 5226 | J-S-80-25-1 9696 | J-S-75-1-7 23,793 | J-S-75-25-6 41,878 |
| | J-S-85-1-7 691 | J-S-85-25-6 4221 | J-S-80-1-7 5459 | J-S-80-25-2 9900 | J-S-75-1-5 38,588 | J-S-75-25-4 41,908 |
| | J-S-85-1-1 1800 | J-S-85-25-7 6185 | J-S-80-1-5 5857 | J-S-80-25-3 10,954 | J-S-75-1-6 72,320 | J-S-75-25-7 48,434 |

^a Rejected as an outlier by Chauvenet's criterion, not included in further analysis.

3.1.4. Strain Evolution

With an extensometer installed on the bottom fiber of the specimen, the longitudinal deformation and strain of the concrete were continuously recorded during the fatigue test. Under fatigue loading, the concrete strain increased non-uniformly with the elapse of loading cycles. This phenomenon was observed in all specimens under different stress levels.

Figure 7 lists the test results from the PC series, including the measured strain-versus-time curves and photos of the failed specimens.

The strain-versus-time curve of a typical plain concrete specimen in Figure 7a can be divided into three stages: the first stage, where the concrete strain increases rapidly at the beginning of loading; the second stage, during which the strain tends to be stable and grows slowly; and the third stage, when approaching the end of loading, where the strain increases rapidly, and the specimen breaks suddenly. The second stage accounts for most of the fatigue life, approximately 80% on average.

The strain amplitude is the difference between the corresponding strains under the maximum and the minimum loads. While the strain amplitude stays stable for most specimens during the fatigue loading cycles, the increase in the strain amplitude is prominent for specimens tested under higher stress levels and whose fatigue life is less than 1000 cycles, as shown in Figure 7a,b. In general, concrete deforms in three stages during the fatigue loading of most PC series specimens, and the smaller the maximum stress level, the more distinctive the three-stage feature. These deformation characteristics are consistent with the three-stage rule of concrete fatigue flexural failure recorded in the literature [7].

Some peculiarities in strain measurement were observed during the fatigue testing. For example, in Figure 7c, the initial rapid strain growth stage was missed in Specimen S-80-1-1 because the first 200 cycles were not recorded due to an operational mistake. Some specimens were recorded with strain–time curves similar to Figure 7d, where a strain reduction occurred after some fatigue cycles. The corresponding failure photos show that in these specimens, concrete failure occurred outside the measuring range

of the extensometer. The range of the extensometer for the PC series was extended to 90 mm. However, the pure bending region was 150 mm (the gauge length was subsequently extended to 146 mm for the RC series). When a specimen cracked outside the measuring range of the extensometer, the corresponding concrete deformation was more significant than that within the measuring range, resulting in the concrete being squeezed and the measured strain decreasing with the increase in loading cycles. Figure 7e,f, for Specimens S-75-25-2 and S-75-1-12, shows strain fluctuation. Because the fatigue test duration was relatively long for specimens with lower stress levels, the machine vibration and other unintentional disturbances may have affected the strain extensometer recording.

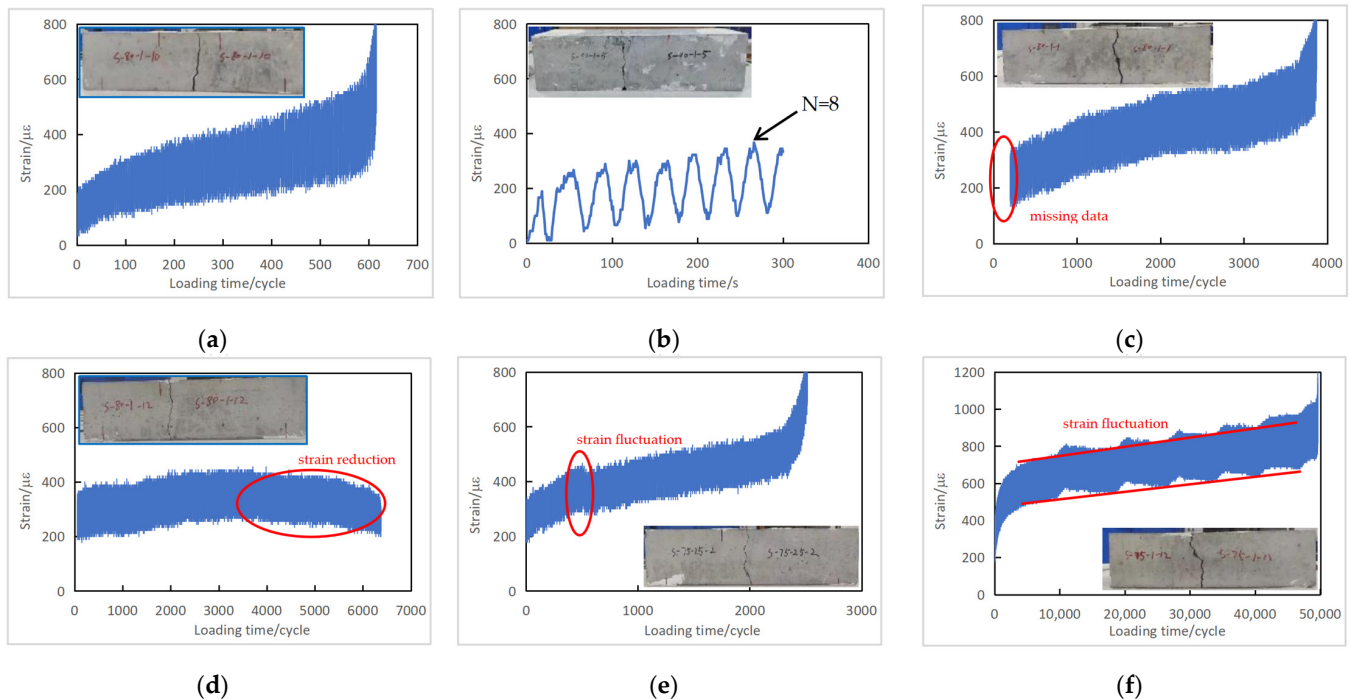


Figure 7. Fatigue strain versus loading time curves of plain concrete specimens (PC series): (a) Specimen S-80-1-10; (b) Specimen S-90-1-5; (c) Specimen S-80-1-1; (d) Specimen S-80-1-12; (e) Specimen S-75-25-2; (f) Specimen S-75-1-12.

For the test specimens whose fracture occurred within the measurement range of the extensometer, the measured minimum and maximum strains during the last cycle of fatigue loading are summarized in Table 7, where the influence of machine vibration on the extensometer measurement has been eliminated. The residual strain, the remaining strain when the load is reduced to 0, was linearly extrapolated from the measured minimum and maximum strains and the applied stresses. The deformation modulus, the slope of the line connecting the loading and unloading tips, of the last fatigue cycle, is also reported.

As seen in Table 7, for specimens with a minimum stress level of 0.10, the maximum strain in the plain concrete specimen during the last fatigue cycle increased from $578 \mu\epsilon$ to $1164 \mu\epsilon$ as the maximum stress level decreased from 0.90 to 0.75. For specimens tested under the same maximum stress level, the minimum strain and the corresponding residual strain at the last fatigue cycle increased as the minimum stress level increased from 0.10 to 0.25, implying more significant fatigue damage with a lower stress ratio. However, the coefficient of variation of the maximum strain, minimum strain, residual strain, and the deformation modulus at failure was large, indicating significant discreteness in the fatigue material properties. This large dispersion may be caused by the discreteness of the concrete material and its static strength [26]. Moreover, measurement error may have influenced the minimum and maximum strains at fatigue failure.

Table 7. Measured strains in plain concrete specimens (PC series) at the end of the fatigue test.

| Specimen Designation | Maximum Strain ($\mu\epsilon$) | Minimum Strain ($\mu\epsilon$) | Residual Strain ($\mu\epsilon$) | Deformation Modulus (MPa) |
|----------------------|-------------------------------------|-------------------------------------|--------------------------------------|------------------------------|
| S-90-1-1 | 789 | 278 | 219 | 9783 |
| S-90-1-5 | 367 | 111 | 84 | 19,531 |
| Mean value | 578 | 194 | 152 | 14,657 |
| C.V. | 0.52 | 0.61 | 0.63 | 0.47 |
| S-90-25-1 | 456 | 222 | 125 | 16,439 |
| S-90-25-2 | 1000 | 522 | 314 | 7788 |
| S-90-25-3 | 1167 | 622 | 395 | 7028 |
| S-90-25-5 | 411 | 289 | 218 | 23,271 |
| Mean value | 758 | 478 | 309 | 12,696 |
| C.V. | 0.50 | 0.36 | 0.29 | 0.72 |
| S-90-4-1 | 656 | 467 | 312 | 11,456 |
| S-90-4-2 | 967 | 511 | 212 | 5968 |
| S-90-4-3 | 989 | 678 | 418 | 8114 |
| S-90-4-4 | 556 | 333 | 141 | 11,912 |
| S-90-4-5 | 389 | 233 | 104 | 19,263 |
| Mean value | 711 | 444 | 237 | 11,343 |
| C.V. | 0.37 | 0.38 | 0.54 | 0.45 |
| S-80-1-1 | 1278 | 767 | 678 | 8002 |
| S-80-1-3 | 733 | 422 | 363 | 12,723 |
| S-80-1-4 | 1344 | 533 | 383 | 3617 |
| S-80-1-5 | 856 | 311 | 210 | 7010 |
| S-80-1-7 | 256 | 122 | 97 | 29,873 |
| S-80-1-9 | 1033 | 578 | 484 | 8176 |
| S-80-1-10 | 1011 | 433 | 312 | 6361 |
| S-80-1-11 | 367 | 200 | 168 | 25,696 |
| S-80-1-12 | 444 | 267 | 232 | 21,218 |
| Mean value | 814 | 404 | 325 | 13,631 |
| C.V. | 0.48 | 0.50 | 0.55 | 0.70 |
| S-75-1-2 | 267 | 156 | 133 | 33,763 |
| S-75-1-7 | 1156 | 500 | 377 | 5786 |
| S-75-1-8 | 733 | 267 | 179 | 8125 |
| S-75-1-9 | 989 | 533 | 444 | 8255 |
| S-75-1-11 | 1878 | 722 | 534 | 3101 |
| S-75-1-12 | 1511 | 944 | 834 | 6676 |
| S-75-1-13 | 1144 | 656 | 559 | 6656 |
| Mean value | 1097 | 423 | 344 | 12,082 |
| C.V. | 0.47 | 0.66 | 0.69 | 0.87 |
| S-75-25-2 | 1222 | 744 | 467 | 5957 |
| S-75-25-4 | 1456 | 922 | 627 | 4876 |
| S-75-25-5 | 1200 | 811 | 588 | 7330 |
| S-75-25-6 | 622 | 422 | 306 | 14,117 |
| S-75-25-7 | 411 | 244 | 143 | 18,599 |
| S-75-25-8 | 1444 | 933 | 676 | 4975 |
| S-75-25-9 | 1741 | 1022 | 528 | 2737 |
| S-75-25-10 | 1100 | 778 | 581 | 9238 |
| S-75-25-11 | 1367 | 856 | 559 | 5118 |
| S-75-25-12 | 1078 | 667 | 437 | 6135 |
| Mean value | 1164 | 740 | 491 | 7908 |
| C.V. | 0.34 | 0.33 | 0.33 | 0.62 |

Note: C.V. stands for coefficient of variation.

The number of cycles when a macroscopic crack was observed on the side surfaces of a reinforced concrete specimen is shown in the figure as a dotted line, and the right end shows when the fatigue test was terminated.

For the typical reinforced concrete specimens shown in Figure 8a–d, the development of fatigue strain was initially consistent with that of the plain concrete specimens: the concrete deformed rapidly at the first stage of loading and gradually stabilized at the second stage. Unlike the plain concrete specimen, the rapid growth of the concrete strain in the third stage was not observed in the RC series. In contrast to the sudden fracture in the PC series once the concrete cracked, concrete cracking in the RC series did not lead to brittle fracture of the beam specimen. This ductile behavior is the consequence of the reinforcement effect. When concrete starts cracking, the tensile stress in the bottom part is sustained by the reinforcement; therefore, concrete strain tends to be stable, limiting the upward propagation of concrete cracks. By the time the fatigue test was terminated beyond the first detection of a macroscopic concrete crack, concrete fatigue strain in the PC series remained in the stable stage of strain development. Also, because of the role of reinforcement after concrete cracking, the strain amplitude in the reinforced concrete specimens did not increase rapidly, even for specimens tested under higher stress levels.

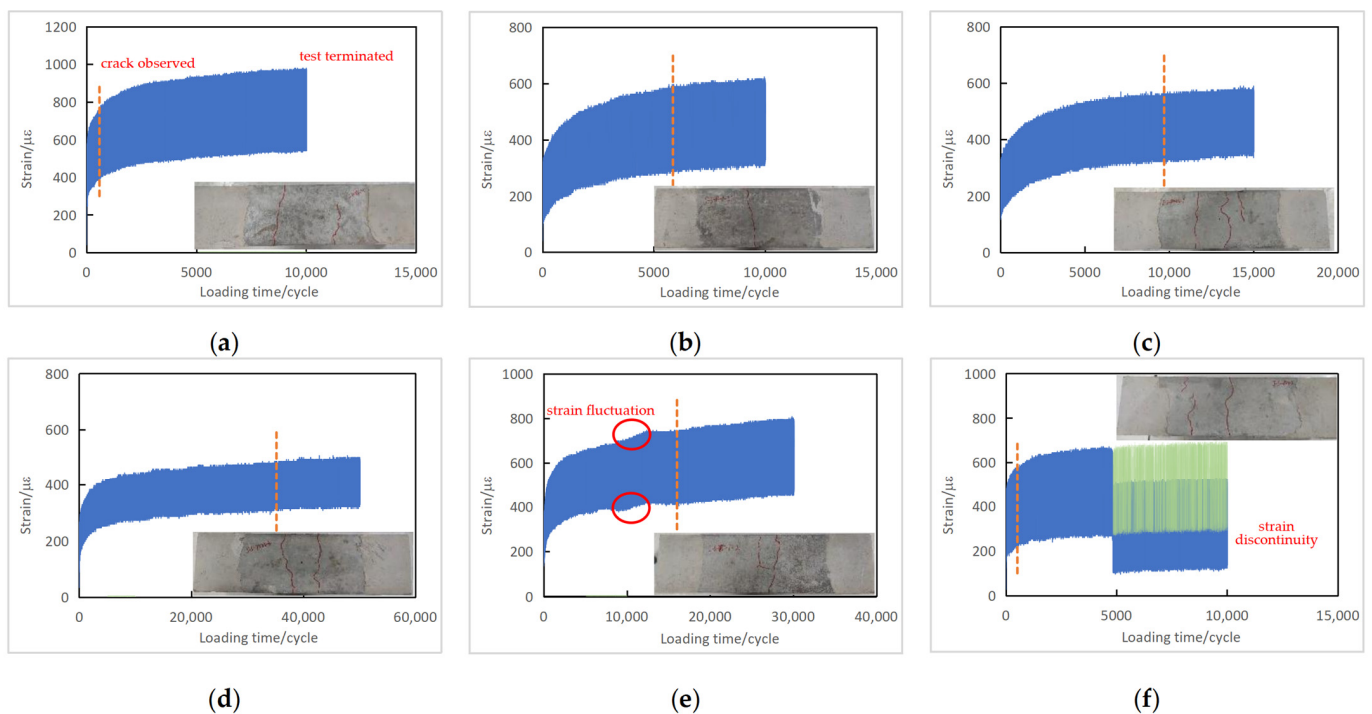


Figure 8. Fatigue strain versus loading time curves of reinforced concrete specimens (RC series): (a) Specimen J-S-85-1-5; (b) Specimen J-S-80-1-5; (c) Specimen J-S-80-25-1; (d) Specimen J-S-75-25-3; (e) Specimen J-S-75-1-2; (f) Specimen J-S-85-1-3.

The strain-versus-time curve in Figure 8e shows the strain fluctuation similarly observed in the PC series. Moreover, Figure 8f, for Specimen J-S-85-1-3, shows an apparent strain discontinuity at about 5000 cycles. This peculiarity is due to an accidental touch to the extensometer. The adjusted strain, shown as the green lines in Figure 8f, was obtained by simply translating the recorded strain data.

To analyze the fatigue strain development in the reinforced concrete specimens, the measured minimum strain, measured maximum strain, and extrapolated residual strain (the remaining strain if the specimen is unloaded to 0) just before fatigue concrete cracking of the specimens are summarized in Table 8.

As observed in Table 8, the fatigue strain of the reinforced concrete specimens evolved similarly to the plain concrete specimens. The maximum strain at failure increased with the decrease in the maximum stress level. However, the maximum strain in the reinforced concrete specimens was generally smaller than that in the plain concrete specimens, which may have

been caused by the existence of reinforcement. Reinforcement can restrict concrete deformation, resulting in a lower maximum strain and coefficient of variation in the RC series.

Table 8. Measured strains in reinforced concrete specimens (RC series) at fatigue cracking initiation.

| Specimen Designation | Maximum Strain ($\mu\epsilon$) | Minimum Strain ($\mu\epsilon$) | Residual Strain ($\mu\epsilon$) | Deformation Modulus (MPa) |
|----------------------|-------------------------------------|-------------------------------------|--------------------------------------|------------------------------|
| J-S-85-1-1 | 562 | 281 | 226 | 12,867 |
| J-S-85-1-2 | 610 | 274 | 219 | 11,362 |
| J-S-85-1-3 | 575 | 212 | 145 | 10,321 |
| J-S-85-1-4 | 486 | 185 | 125 | 12,299 |
| J-S-85-1-5 | 767 | 397 | 331 | 10,202 |
| J-S-85-1-6 | 788 | 274 | 177 | 7268 |
| J-S-85-1-7 | 664 | 295 | 226 | 10,166 |
| Mean value | 636 | 274 | 207 | 10,641 |
| C.V. | 0.17 | 0.25 | 0.33 | 0.17 |
| J-S-85-25-1 | 726 | 432 | 295 | 10,322 |
| J-S-85-25-2 | 685 | 432 | 314 | 11,996 |
| J-S-85-25-3 | 801 | 493 | 350 | 9863 |
| J-S-85-25-4 | 685 | 418 | 293 | 11,430 |
| J-S-85-25-5 | 658 | 418 | 309 | 12,848 |
| J-S-85-25-6 | 466 | 260 | 168 | 15,030 |
| J-S-85-25-7 | 644 | 445 | 309 | 13,484 |
| Mean value | 666 | 414 | 291 | 12,139 |
| C.V. | 0.15 | 0.18 | 0.20 | 0.15 |
| J-S-80-1-1 | 432 | 130 | 78 | 11,875 |
| J-S-80-1-2 | 541 | 233 | 175 | 11,467 |
| J-S-80-1-3 | 925 | 493 | 410 | 8153 |
| J-S-80-1-4 | 870 | 479 | 404 | 9013 |
| J-S-80-1-5 | 589 | 295 | 244 | 12,201 |
| J-S-80-1-6 | 897 | 575 | 388 | 8638 |
| J-S-80-1-7 | 568 | 336 | 294 | 15,204 |
| Mean value | 689 | 363 | 285 | 10,936 |
| C.V. | 0.29 | 0.44 | 0.45 | 0.23 |
| J-S-80-25-1 | 555 | 329 | 219 | 12,601 |
| J-S-80-25-2 | 1055 | 753 | 598 | 9142 |
| J-S-80-25-3 | 692 | 452 | 332 | 11,689 |
| J-S-80-25-5 | 658 | 452 | 337 | 12,873 |
| J-S-80-25-6 | 740 | 514 | 386 | 11,718 |
| J-S-80-25-7 | 411 | 281 | 206 | 20,139 |
| Mean value | 685 | 463 | 346 | 13,027 |
| C.V. | 0.31 | 0.36 | 0.41 | 0.29 |
| J-S-75-1-1 | 808 | 507 | 448 | 10,942 |
| J-S-75-1-2 | 740 | 418 | 368 | 10,775 |
| J-S-75-1-3 | 973 | 651 | 601 | 10,780 |
| J-S-75-1-4 | 712 | 384 | 334 | 10,582 |
| J-S-75-1-5 | 315 | 116 | 78 | 16,540 |
| J-S-75-1-6 | 733 | 452 | 409 | 12,364 |
| J-S-75-1-7 | 630 | 438 | 409 | 18,078 |
| Mean value | 702 | 424 | 378 | 12,866 |
| C.V. | 0.29 | 0.38 | 0.42 | 0.24 |
| J-S-75-25-3 | 486 | 322 | 240 | 16,237 |
| J-S-75-25-4 | 603 | 418 | 325 | 14,428 |
| J-S-75-25-5 | 747 | 500 | 377 | 10,826 |
| J-S-75-25-6 | 849 | 610 | 493 | 11,286 |
| J-S-75-25-7 | 452 | 281 | 195 | 15,588 |
| Mean value | 627 | 426 | 326 | 13,673 |
| C.V. | 0.27 | 0.31 | 0.36 | 0.18 |

Note: C.V. stands for coefficient of variation.

3.1.5. Cyclic Stress–Strain Curves

A continuous cyclic stress-versus-strain curve can be obtained, with stress as the ordinate and strain as the abscissa. The measured cyclic stress–strain curves of typical plain concrete specimens are shown in Figure 9.

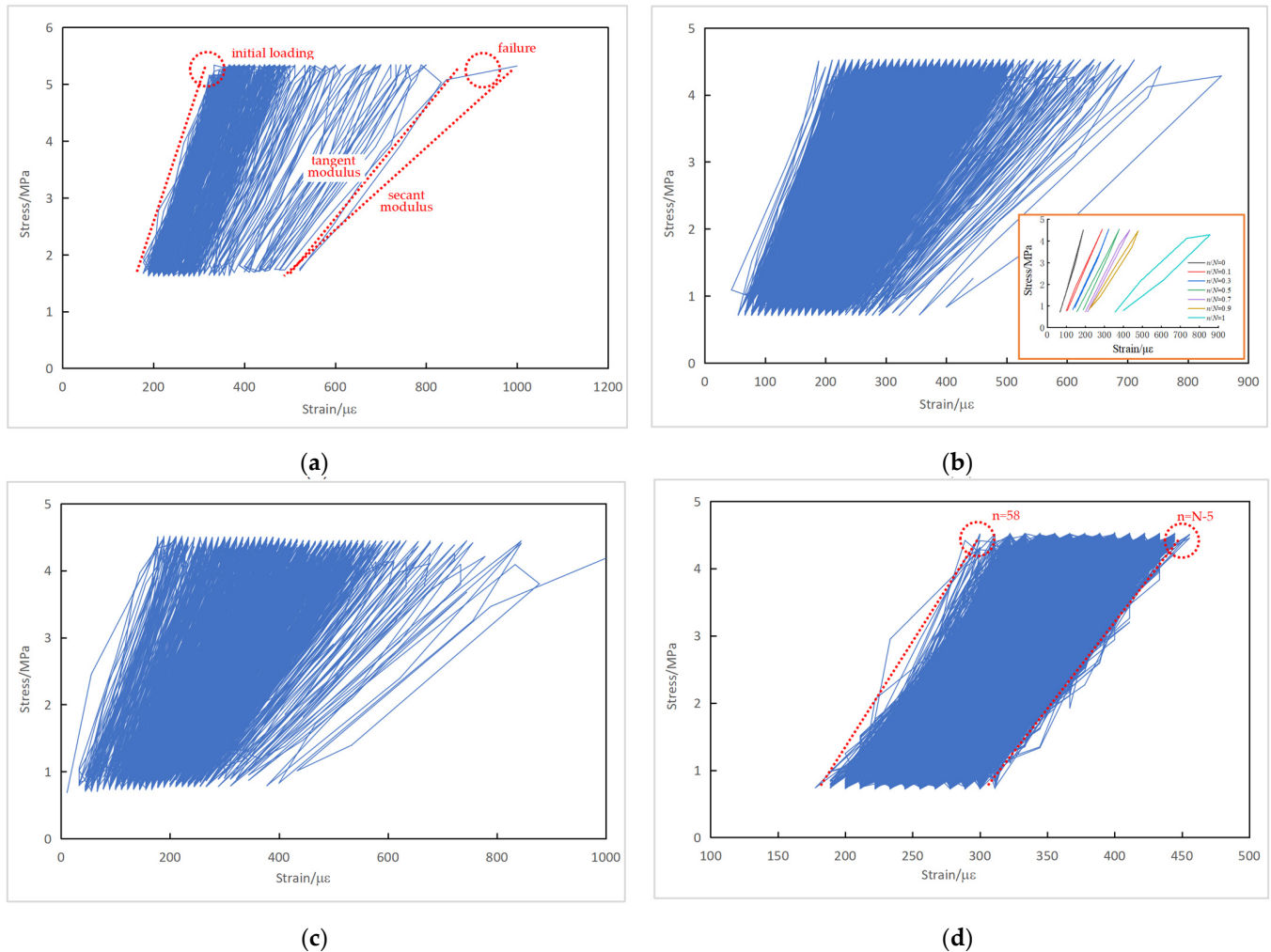


Figure 9. Cyclic stress–strain curves of plain concrete specimens: (a) Specimen S-90-25-2; (b) Specimen S-80-1-5; (c) Specimen S-80-1-10; (d) Specimen S-80-1-12.

Since the fatigue test was under load control, both the maximum and minimum stresses remained constant during fatigue loading. As shown in Section 3.1.4, the strain responses due to fatigue loading kept increasing. The cyclic stress–strain curves in Figure 9 thus demonstrate the evolution of the concrete’s response from the beginning towards the end of the fatigue test. The slope of the cyclic stress–strain curve, termed the deformation modulus of concrete, decreased with the application of fatigue loading. A remarkable decrease in the deformation modulus and differentiation between the tangent and secant modulus was observed before fatigue failure. Figure 9d seems to be an exception, as the strain data of the first 57 and last 5 cycles were not recorded due to operation mistakes. This figure demonstrates that the deformation modulus exhibited a typically three-stage evolution in which the stiffness response was reasonably stable during stage II.

The stress–strain curves at the specified cycle ratio n/N are also depicted in Figure 9b to illustrate the stress–strain evolution more clearly, where n is the number of fatigue loading cycles and N is the total fatigue life. During the earlier stages of fatigue loading, the stress–strain response became more linear elastic. With the increase in the cycle ratio,

plastic damage in the concrete accumulated gradually. As the fatigue loading continued, the loading and unloading branch in a cycle tended to form a hysteresis loop. The area of the hysteresis loop, to some extent, represents the strain energy consumed by the concrete and the fatigue damage accrued during each fatigue loading cycle.

The measured cyclic stress–strain curves of typical reinforced concrete specimens are shown in Figure 10.

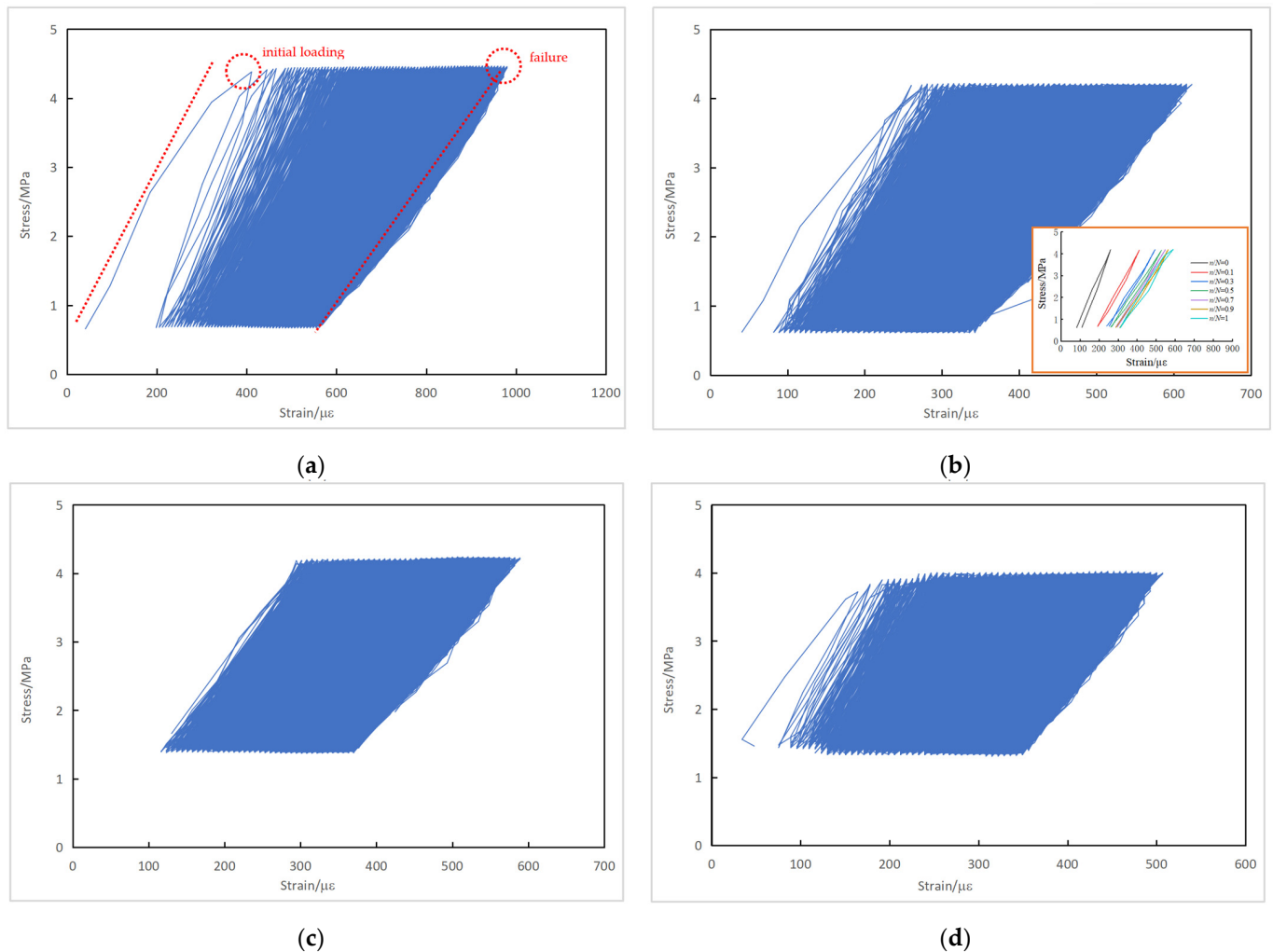


Figure 10. Cyclic stress–strain curves of reinforced concrete specimens: (a) Specimen J-S-85-1-5; (b) Specimen J-S-80-1-5; (c) Specimen J-S-80-25-1; (d) Specimen J-S-75-25-3.

Similarly, the cyclic stress–strain curves of the reinforced concrete specimens show a decrease in the deformation modulus as the fatigue loading continued. Because of restraint from the reinforcement, the decreasing trend in the concrete deformation modulus and specimen stiffness in the reinforced concrete specimens with the number of loading cycles was less noticeable compared to the plain concrete specimens. While a significant decrease in the deformation modulus within the last 10% of fatigue life for the PC series is evident in Figure 9b, Figure 10b shows that the change in the deformation modulus of the RC series was marginal when n/N increased from 0.5 to 1.

3.2. Probabilistic Analysis of Fatigue S-N Curves

3.2.1. Probabilistic Distribution of Fatigue Life

In Section 3.1.3, three specimens tested at S_{\max} of 0.65 did not fail after 1 million cycles and were termed run-outs. Four outliers in Tables 5 and 6 of the fatigue life data were

identified by employing Chauvenet’s criterion [27]. These data points were excluded from further examination. Statistical analysis on two datasets of specimens was performed. One dataset of specimens comprised specimens tested at a fixed minimum stress level of 0.10; the other dataset consisted of specimens tested at varying minimum stress levels, and therefore, the effect of the stress ratio could be considered. Figure 11 shows the Weibull distribution test of the fatigue life of the plain concrete and reinforced concrete specimens, and the corresponding regression analysis results are listed in Table 9. It is worth emphasizing that the equivalent fatigue life was adopted when considering the stress ratio. The slope and intercept terms in the linear equations presented in Figure 11 correspond to the shape parameter m and $\ln t_0$ in Equations (3) and (5), respectively.

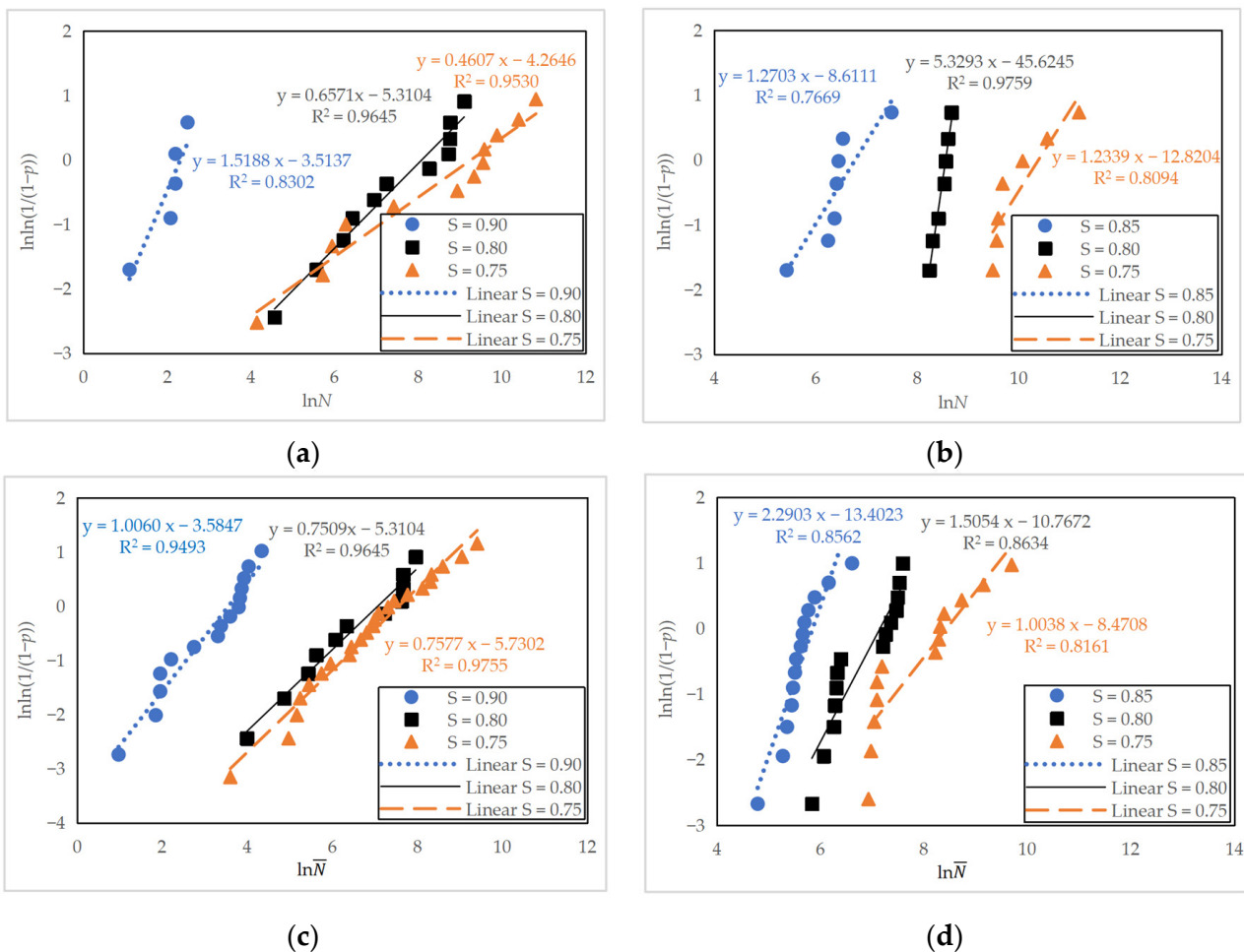


Figure 11. Weibull distribution test of fatigue life: (a) Plain concrete specimens (PC series) at a fixed minimum stress level of 0.10; (b) reinforced concrete specimens (RC series) at a fixed minimum stress level of 0.10; (c) plain concrete specimens (PC series) at varying minimum stress levels; (d) reinforced concrete specimens (RC series) at varying minimum stress levels.

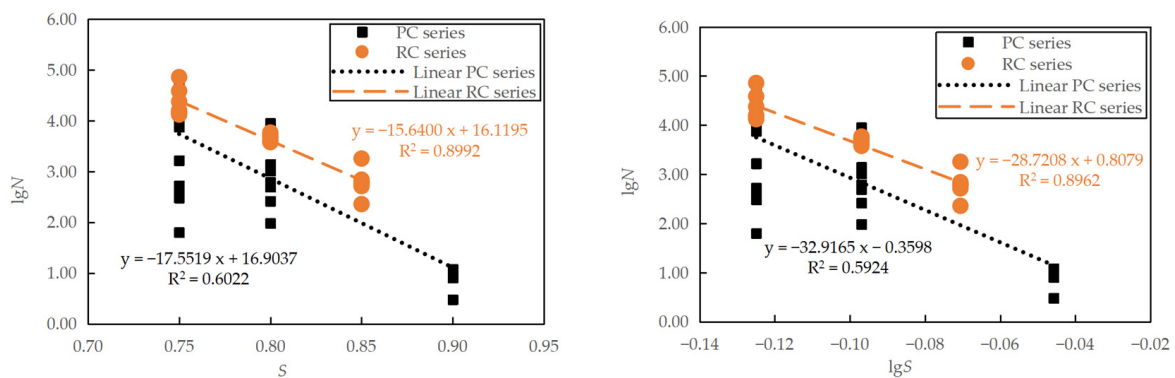
It can be seen in Figure 11 and Table 9 that the coefficient of determination was generally higher for specimens with varying minimum stress levels where more data points were available. Under each stress level, the coefficient of determination exceeded 0.75, indicating a linear relationship between $\ln \ln(1/(1 - p))$ and $\ln N$ (or $\ln \bar{N}$). Therefore, both the fatigue life and equivalent fatigue life correlate reasonably well with the two-parameter Weibull distribution. A linear regression analysis of the fatigue equations is thus presented in the following sections.

Table 9. Regression analysis results of Weibull distribution test.

| Minimum Stress Level | Series | Maximum Stress Level | Number of Specimens | Regression Coefficient m | Regression Coefficient $\ln t_0$ | Coefficient of Determination R^2 |
|-----------------------------------|--------|----------------------|---------------------|----------------------------|----------------------------------|------------------------------------|
| Fixed at 0.10 | PC | 0.90 | 5 | 1.5188 | 3.5137 | 0.83 |
| | | 0.80 | 11 | 0.6571 | 5.3104 | 0.96 |
| | | 0.75 | 12 | 0.4607 | 4.2646 | 0.95 |
| | RC | 0.85 | 7 | 1.2703 | 8.6111 | 0.77 |
| | | 0.80 | 7 | 5.3293 | 45.6245 | 0.98 |
| | | 0.75 | 7 | 1.2339 | 12.8204 | 0.81 |
| Varying (stress ratio considered) | PC | 0.90 | 15 | 1.0060 | 3.5847 | 0.95 |
| | | 0.80 | 11 | 0.7509 | 5.3104 | 0.96 |
| | | 0.75 | 23 | 0.7577 | 5.7302 | 0.98 |
| | RC | 0.85 | 14 | 2.2903 | 13.4023 | 0.86 |
| | | 0.80 | 14 | 1.5054 | 10.7672 | 0.86 |
| | | 0.75 | 13 | 1.0038 | 8.4708 | 0.82 |

3.2.2. Mean Fatigue S-N Curves

When the minimum stress level was fixed as 0.10, the fitting of the plain concrete (PC series) and reinforced concrete (RC series) fatigue test results to the fatigue S-N curves are shown in Figure 12. Note that the constant terms in the linear equations presented in the figure were obtained from the regression analysis of the fatigue life as dependent variable y and the stress level as independent variable x. The constants a, b, A, and B in Equations (6) and (7) were then obtained from simple transformation.



PC series: $S = 0.9631 - 0.0570 \lg N, R^2 = 0.60$

RC series: $S = 1.0307 - 0.0639 \lg N, R^2 = 0.90$

PC series: $\lg S = -0.0109 - 0.0304 \lg N, R^2 = 0.59$

RC series: $\lg S = 0.0281 - 0.0348 \lg N, R^2 = 0.90$

(a)

(b)

Figure 12. Mean fatigue equations at a fixed minimum stress level of 0.10: (a) semi-logarithmic equation; (b) logarithmic equation.

It can be seen in Figure 12 that under the conditions of a fixed minimum stress level, the fatigue equation fitting of the RC series specimens was reasonably good, with the R^2 close to 0.90. However, the R^2 of the PC series was about 0.60, which indicates that only 60% of the variation in N can be explained by the regression relationship. Large discreteness can be observed between the PC specimens with the same stress level, particularly at a lower stress level of 0.75. The reinforced concrete specimens show a slightly longer fatigue life than the plain concrete counterparts, indicating that although reinforcement mainly controlled the fatigue crack propagation in the reinforced components, the existence of reinforcement did affect the flexural fatigue cracking of concrete beneficially.

By taking the logarithm of S and substituting S with the semi-logarithmic fatigue equation, a relationship between $\lg S$ and $\lg N$ can be obtained, that is, $\lg S = \lg (0.9631 - 0.0570 \lg N)$ for the PC series and $\lg S = \lg (1.0307 - 0.0639 \lg N)$ for the RC series, which can then be compared with the logarithmic fatigue equations, as shown in Figure 13. The two equations are equivalent to each other for the stress levels studied. However, when it is necessary to extend the stress level S to a lower value of less than 0.70, the logarithmic fatigue equation predicts a fatigue life longer than the semi-logarithmic fatigue equation. This observation is consistent with previous research [7].

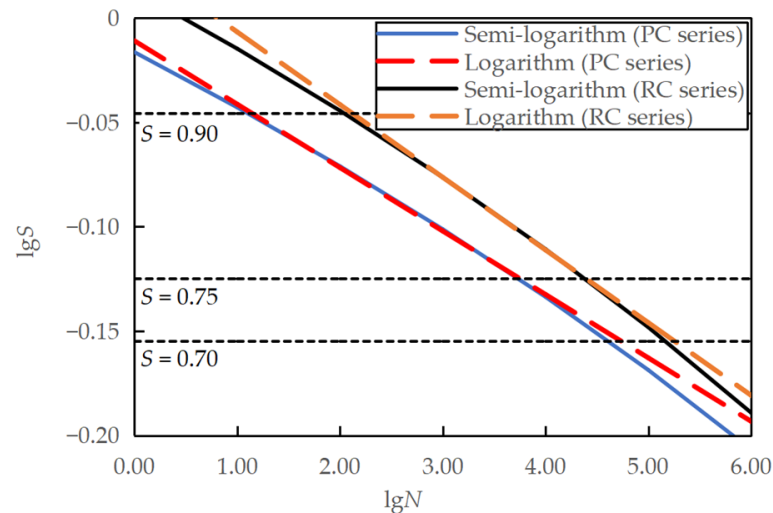
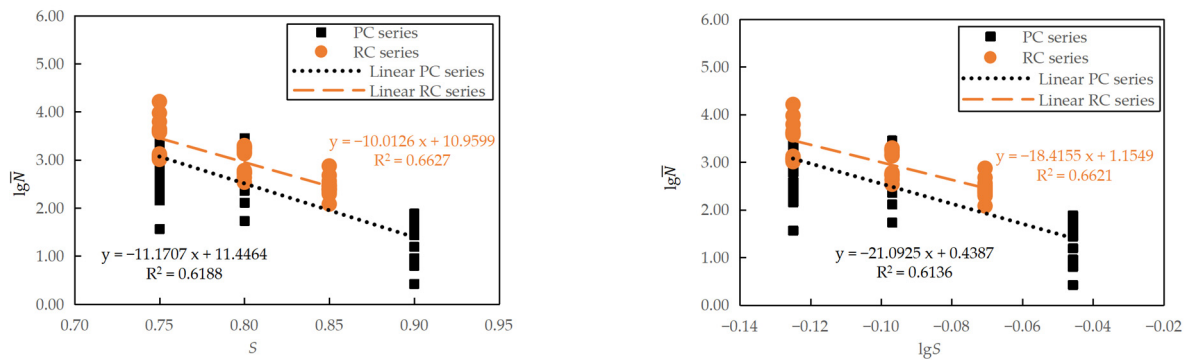


Figure 13. Comparison between semi-logarithmic and logarithmic equations for specimens tested at a fixed minimum stress level of 0.10.

The maximum stress level S was also taken as an independent variable when considering the influence of the stress ratio R . Similar to Section 3.2.1, the equivalent fatigue life \bar{N} , which relates to the stress ratio R and fatigue life N as $\bar{N} = N^{1-R}$, is used to combine all experimental data at the same maximum stress level [9]. This \bar{N} is then treated as the dependent variable in regression analysis, making fitting linear fatigue equations convenient in practical applications. The regression analysis of semi-logarithmic and logarithmic fatigue equations, considering the effect of the stress ratio, of the plain and reinforced concrete specimens are shown in Figure 14. The figure also shows the corresponding linear regression equations, from which the constants a , b , A , and B in Equations (8) and (9) were obtained through simple transformation.

It can be seen in Figure 14 that when considering the stress ratio R , the fatigue equations of the plain and reinforced concrete specimens are comparable, with the RC series showing a slightly longer fatigue life. However, the coefficients of determination of the fitted equations are not high (0.61~0.66). This low linearity correlation reflects the complexity of the concrete fatigue phenomenon, especially in the sense of significant variation.

Similarly, by taking the logarithm of S and substituting S with the semi-logarithmic fatigue equation, a relationship between $\lg S$ and $\lg N$ can be obtained, that is, $\lg S = \lg (1.0247 - 0.0895 \lg \bar{N})$ for the PC series and $\lg S = \lg (1.0946 - 0.0999 \lg \bar{N})$ for the RC series, which can then be compared with the logarithmic fatigue equations, as shown in Figure 15. The two equations were identical for the studied stress levels. However, the logarithmic fatigue equation predicted a longer fatigue life than the semi-logarithmic fatigue equation for stress levels smaller than 0.70.



PC series: $S = 1.0247 - 0.0895(1 - R) \lg N, R^2 = 0.62$ PC series: $\lg S = 0.0208 - 0.0474(1 - R) \lg N, R^2 = 0.61$
 RC series: $S = 1.0946 - 0.0999(1 - R) \lg N, R^2 = 0.66$ RC series: $\lg S = 0.0627 - 0.0543(1 - R) \lg N, R^2 = 0.66$

(a)

(b)

Figure 14. Mean fatigue equations considering the effect of stress ratio: (a) semi-logarithmic equation; (b) logarithmic equation.

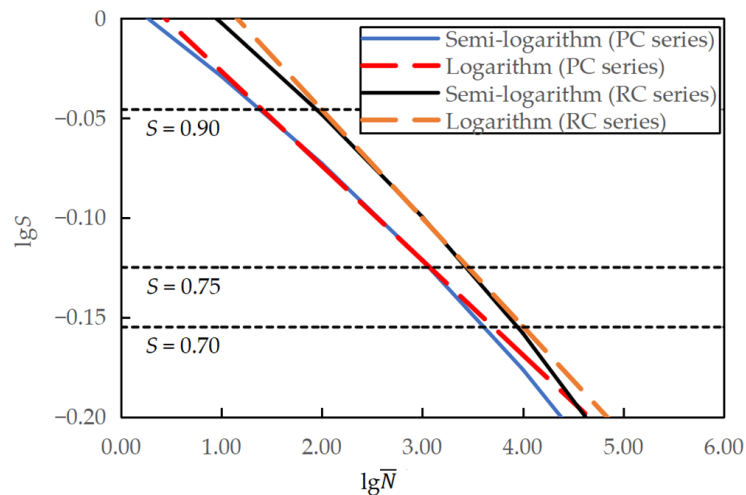


Figure 15. Comparison between semi-logarithmic and logarithmic equations for specimens tested at varying minimum stress levels.

The mean fatigue $S-N$ curves from this study are summarized in Table 10.

Table 10. Summary of mean fatigue $S-N$ equations.

| Series | Analyzed Specimens | Semi-Logarithmic Equations | Logarithmic Equations |
|--------|-------------------------------------|------------------------------------|--|
| PC | Constant $S_{\min} = 0.10$ | $S = 0.9631 - 0.0570 \lg N$ | $\lg S = -0.0109 - 0.0304 \lg N$ |
| | Varying S_{\min} , R considered | $S = 1.0247 - 0.0895(1 - R) \lg N$ | $\lg S = 0.0208 - 0.0474(1 - R) \lg N$ |
| RC | Constant $S_{\min} = 0.10$ | $S = 1.0307 - 0.0639 \lg N$ | $\lg S = 0.0281 - 0.0348 \lg N$ |
| | Varying S_{\min} , R considered | $S = 1.0946 - 0.0999(1 - R) \lg N$ | $\lg S = 0.0627 - 0.0543(1 - R) \lg N$ |

3.2.3. Probabilistic Fatigue $S-N$ Curves

The regression analysis in Section 3.2.2 obtained fatigue equations corresponding to a failure probability of approximately 50%. By substituting the regression parameters m and t_0 from Table 9 into Equation (10), the fatigue life and equivalent fatigue life under different failure probabilities at various stress levels for the plain concrete specimens (PC series) and reinforced concrete specimens (RC series) was obtained and are listed in Table 11.

Table 11. Fatigue life (and equivalent fatigue life \bar{N} when considering R) in cycles at various failure probabilities.

| Analyzed Specimens | Failure Probability p | PC Series | | | RC Series | | |
|---------------------------------------|-------------------------|----------------------|------|------|----------------------|------|--------|
| | | Maximum Stress Level | | | Maximum Stress Level | | |
| | | 0.90 | 0.80 | 0.75 | 0.85 | 0.80 | 0.75 |
| Constant $S_{min} = 0.10$ | 0.1 | 2 | 105 | 79 | 149 | 3425 | 5252 |
| | 0.2 | 4 | 330 | 404 | 270 | 3943 | 9648 |
| | 0.3 | 5 | 674 | 1118 | 390 | 4305 | 14,110 |
| | 0.4 | 6 | 1164 | 2437 | 518 | 4606 | 18,878 |
| | 0.5 | 8 | 1852 | 4728 | 659 | 4877 | 24,176 |
| Varying S_{min} , R considered | 0.1 | 4 | 59 | 99 | 130 | 286 | 491 |
| | 0.2 | 8 | 160 | 266 | 181 | 472 | 1037 |
| | 0.3 | 13 | 299 | 494 | 222 | 644 | 1655 |
| | 0.4 | 18 | 482 | 793 | 259 | 817 | 2367 |
| | 0.5 | 25 | 723 | 1187 | 296 | 1001 | 3209 |

The data in Table 11 are fitted to semi-logarithmic Equations (6) and (8) and logarithmic Equations (7) and (9), respectively, and the regression coefficients a , b , A , and B under different failure probability p were obtained. The values are shown in Table 12. The smallest R^2 value of the regression analysis was obtained as 0.83 under a failure probability of 0.1, indicating a linear relationship between S (or $\lg S$ for logarithmic equation) and $\lg N$. Comparing Tables 10 and 12, probabilistic fatigue equations derived in this section with a failure probability of 0.5 are very close to those developed in Section 3.2.2, indicating the validity of probabilistic analysis.

Table 12. Coefficients from regression analysis of probabilistic fatigue equations.

| Analyzed Specimens | Series | Failure Probability p | Semi-Logarithmic Equations | | | Logarithmic Equations | | | |
|---------------------------------------|--------|-------------------------|----------------------------|-----------------------|------------------------------------|---------------------------|-----------------------|------------------------------------|---------|
| | | | Intercept Coefficient a | Slope Coefficient b | Coefficient of Determination R^2 | Intercept Coefficient A | Slope Coefficient B | Coefficient of Determination R^2 | |
| | | | Constant $S_{min} = 0.10$ | PC | 0.1 | 0.9446 | 0.0896 | 0.85 | -0.0213 |
| | | 0.2 | 0.9488 | 0.0696 | 0.92 | -0.0192 | 0.0368 | 0.90 | |
| | | 0.3 | 0.9506 | 0.0610 | 0.94 | -0.0183 | 0.0323 | 0.93 | |
| | | 0.4 | 0.9517 | 0.0558 | 0.95 | -0.0178 | 0.0295 | 0.94 | |
| | | 0.5 | 0.9525 | 0.0520 | 0.96 | -0.0174 | 0.0275 | 0.95 | |
| | RC | 0.1 | 1.0034 | 0.0647 | 0.84 | 0.0140 | 0.0355 | 0.83 | |
| | | 0.2 | 1.0148 | 0.0644 | 0.92 | 0.0200 | 0.0352 | 0.91 | |
| | | 0.3 | 1.0220 | 0.0642 | 0.96 | 0.0237 | 0.0350 | 0.96 | |
| | | 0.4 | 1.0274 | 0.0640 | 0.98 | 0.0265 | 0.0349 | 0.98 | |
| | | 0.5 | 1.0320 | 0.0639 | 1.00 | 0.0288 | 0.0348 | 0.99 | |
| Varying S_{min} , R considered | PC | 0.1 | 0.9641 | 0.1019 | 0.97 | -0.0113 | 0.0538 | 0.96 | |
| | | 0.2 | 0.9909 | 0.0946 | 0.96 | 0.0029 | 0.0500 | 0.95 | |
| | | 0.3 | 1.0058 | 0.0905 | 0.96 | 0.0107 | 0.0478 | 0.95 | |
| | | 0.4 | 1.0163 | 0.0876 | 0.96 | 0.0163 | 0.0463 | 0.95 | |
| | | 0.5 | 1.0248 | 0.0853 | 0.95 | 0.0208 | 0.0451 | 0.94 | |
| | | RC | 0.1 | 1.2199 | 0.1734 | 0.99 | 0.1313 | 0.0945 | 0.98 |
| | | | 0.2 | 1.1490 | 0.1318 | 1.00 | 0.0925 | 0.0717 | 0.99 |
| | | | 0.3 | 1.1197 | 0.1146 | 1.00 | 0.0765 | 0.0623 | 1.00 |
| | | | 0.4 | 1.1020 | 0.1041 | 1.00 | 0.0668 | 0.0566 | 1.00 |
| | | | 0.5 | 1.0893 | 0.0967 | 1.00 | 0.0599 | 0.0526 | 1.00 |

The fatigue equations of the plain concrete specimens under different failure probabilities are also shown in Figure 16. It is demonstrated in the figure that the lower the failure probability, the shorter the fatigue life at a given stress level. Similarly, semi-logarithmic and logarithmic equations were identical for the stress levels most likely encountered in practical applications. When considering the stress ratio, the slope coefficients are more

stable, and the intercept coefficients are more evenly distributed. Probabilistic $S-N$ curves have similar slopes, but the intercept increases with higher failure probability [9].

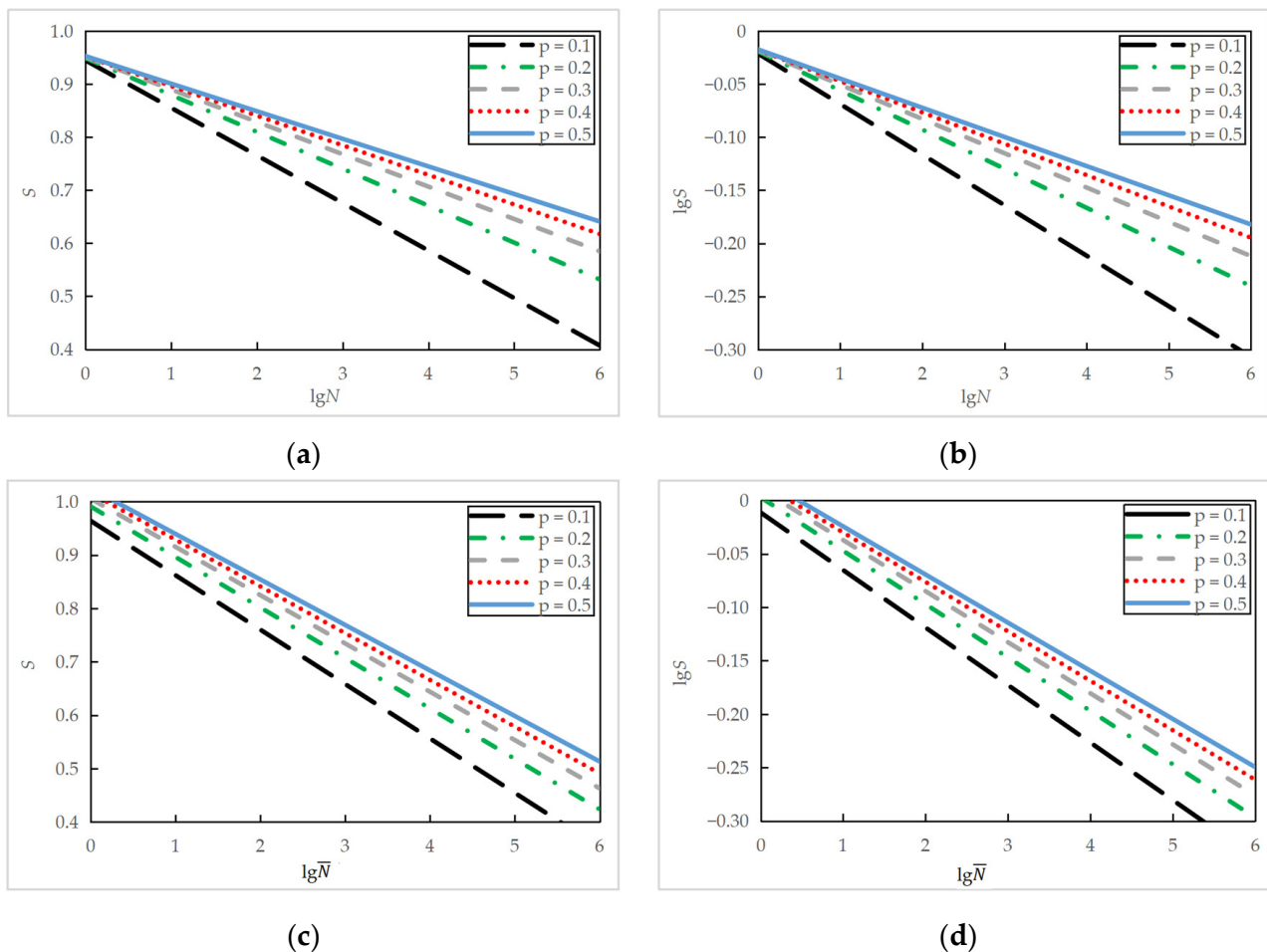


Figure 16. Fatigue $S-N$ equations of PC series under different failure probabilities: (a) semi-logarithmic equation at a fixed minimum stress level of 0.10; (b) logarithmic equation at a fixed minimum stress level of 0.10; (c) semi-logarithmic equation when considering stress ratio; (d) logarithmic equation when considering stress ratio.

3.2.4. Comparison between Fatigue Equations

In this section, we compare the fatigue equations obtained from the experimental investigation with those proposed by other scholars based on their fatigue test results. Since probabilistic fatigue equations are not available explicitly in the literature, only the mean fatigue equations were analyzed. Similarly, the comparison focuses on the fatigue analysis results of the plain concrete specimens.

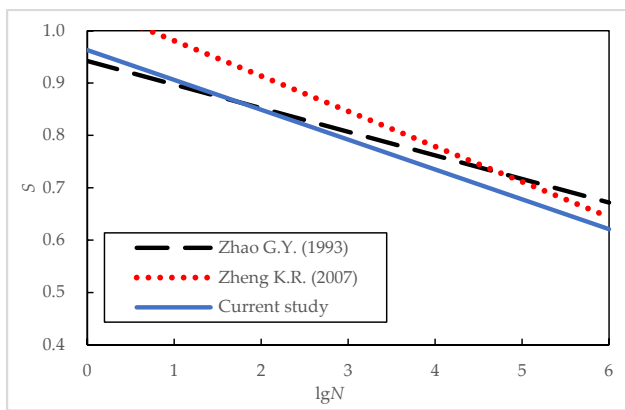
When the minimum stress level was fixed at 0.10, the fatigue equations of the plain concrete specimens obtained in the current study were compared with those proposed in References [7,8,13]. A summary of the various fatigue test programs along with the obtained fatigue equations are shown in Table 13, and a graphic representation of the equations is shown in Figure 17. It should be noted that the test condition in Reference [8] was three-point bending.

As can be seen in Figure 17, the fatigue equation proposed in the current work is relatively close to those proposed in the literature. For most fatigue problems in bridge engineering, the fatigue life of concrete usually lies within the range of 100~100,000 cycles, and the maximum stress levels are between 0.70 and 0.85. Compared to the high-strength concrete in References [7,8,13], the normal-grade C50 concrete in this study had a lower

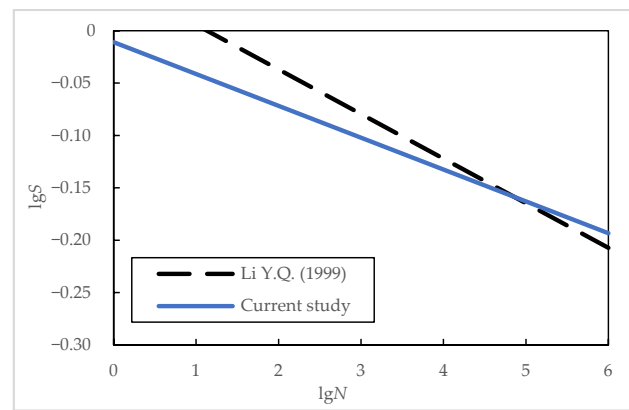
static flexural strength f and slightly lower fatigue strength. The large discreteness of the test results observed in the test program might have caused some discrepancies. The difference in the $S-N$ curves' slope in Figure 17b was probably caused by the difference in the test set-up. Under three-point bending, shear force exists at the cross-section where the beam specimen bears the maximum bending moment. The combined effect of the shear force and the bending moment causes more severe conditions, thus causing the slope of the fatigue equation proposed in Reference [8] to be steeper.

Table 13. Comparison of fatigue equations obtained for a fixed minimum stress level of 0.10.

| Reference | f (MPa) | Specimen Dimension (cm) | Number of Datapoints | S_{min} | S_{max} | Test Condition | Test Frequency (Hz) | Fatigue Equations |
|------------------------|-----------|-------------------------|----------------------|-----------|-----------|---------------------|---------------------|---|
| Zhao G.Y. (1993) [7] | 7.43 | 10 × 10 × 40 | 16 | 0.10 | 0.70~0.90 | Four-point bending | 5~10 | $S = 0.942 - 0.045 \lg N$ |
| Li Y.Q. (1999) [8] | 7.68 | 10 × 10 × 51.5 | 60 | 0.10 | 0.60~0.90 | Three-point bending | 10 | $\lg S = 0.0483 - 0.0426 \lg N$ |
| Zheng K.R. (2007) [13] | 7.6 | 10 × 10 × 40 | 57 | 0.10 | 0.65~0.90 | Four-point bending | 2~10 | $S = 1.04808 - 0.0673 \lg N$ |
| Current study | 5.6 | 15 × 15 × 55 | 28 | 0.10 | 0.75~0.90 | Four-point bending | 0.1~5 | $S = 0.9631 - 0.0570 \lg N$ $\lg S = -0.0109 - 0.0304 \lg N$ |



(a)



(b)

Figure 17. Comparison of fatigue equations at a fixed minimum stress level of 0.10: (a) semi-logarithmic equations; (b) logarithmic equations [7,8,13].

When the effect of the stress ratio R is considered, the fatigue equations of the plain concrete specimens obtained in the current study were compared with those proposed in References [9,10]. A summary of various fatigue test programs and the obtained fatigue equations are shown in Table 14. A graphic representation of these equations is shown in Figure 18.

Table 14. Comparison of fatigue equations considering the effect of stress ratio R .

| Reference | f (MPa) | Specimen Dimension (cm) | Number of Datapoints | R | S_{max} | Test Condition | Test Frequency (Hz) | Fatigue Equations |
|---------------------|-----------|-------------------------|----------------------|-----------|-----------|--------------------|---------------------|--|
| Shi X.P. (1990) [9] | 6.08 | 10 × 10 × 50 | 73 | 0.08~0.5 | 0.55~0.90 | Four-point bending | 1~20 | $S = 0.999 - 0.0722(1 - R) \lg N$ $\lg S = 0.0162 - 0.0422(1 - R) \lg N$ |
| Wu Y.Q. (2005) [10] | 5.1 | 10 × 10 × 40 | 84 | 0.1~0.5 | 0.625~0.9 | Four-point bending | 1~20 | $\lg S = 0.0044 - 0.045(1 - R) \lg N$ |
| Current study | 5.6 | 15 × 15 × 55 | 49 | 0.11~0.44 | 0.75~0.90 | Four-point bending | 0.1~5 | $S = 1.0247 - 0.0895(1 - R) \lg N$ $\lg S = 0.0208 - 0.0474(1 - R) \lg N$ |

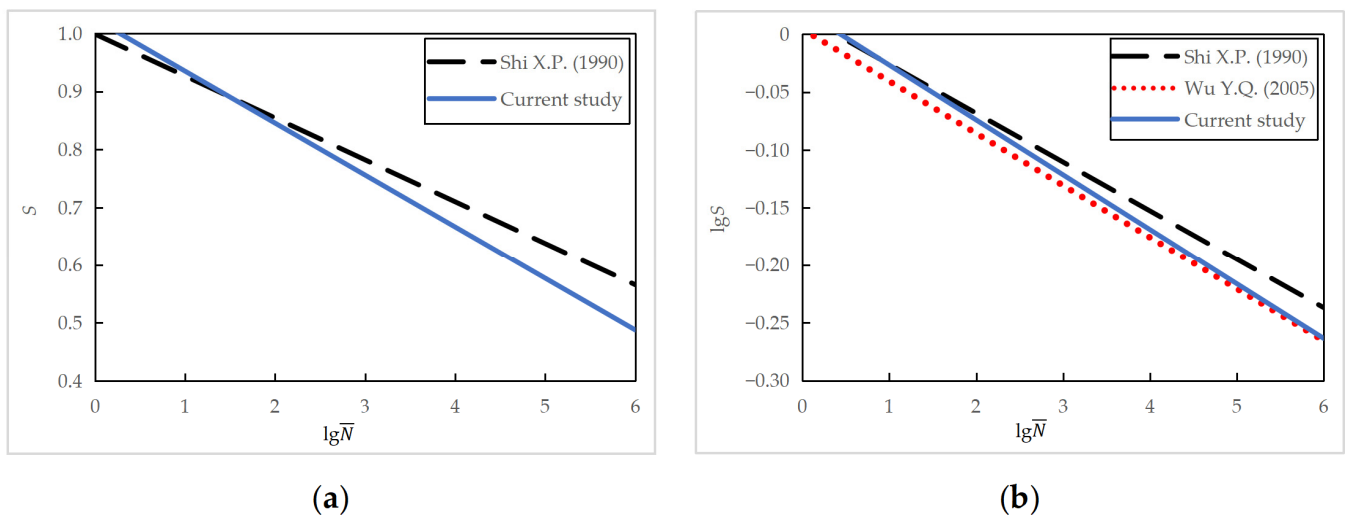


Figure 18. Comparison of fatigue equations considering the effect of stress ratio: (a) semi-logarithmic equations; (b) logarithmic equations [9,10].

It can be seen in Table 14 and Figure 18 that the fatigue equations from three sources had slight differences in their slope and intercept coefficients. The fatigue equation proposed in the current work lies between those in References [9,10] for the range of stress levels and fatigue life of practical concern. Note that the static flexural strength f of three batches of concrete was relatively close. In short, the difference between the fatigue equations obtained from similar test conditions when considering the effect of the stress ratio is slight. Regarding the influencing factors for the fatigue characteristics of concrete, both the maximum stress level and stress ratio are essential parameters, followed by the influence of the concrete strength grade, with slightly less significance. This observation confirms the conclusions from earlier research [28].

3.3. Future Research

Large discreteness in the fatigue life and longitudinal strain of concrete was observed for specimens tested under the same stress conditions, even in carefully controlled fatigue tests. This large discreteness was partly caused by imperfections in the fatigue testing machine and measuring techniques. It also reflects that concrete fatigue is a complicated problem, and deep understanding of the important affecting parameters and the failure mechanism still needs to be improved. With upgraded test facilities, more fatigue tests with lower stress levels (0.65~0.75) and possibly extending the fatigue loading up to 2 million cycles are desirable in future investigations.

The longitudinal strain in nearly 100 concrete specimens was continuously recorded during the fatigue test. The maximum strain just before fatigue failure was analyzed. Much work is required to utilize the collected strain data fully. For example, the evolution of the maximum, minimum, residual strains, and strain amplitude during the entire process of fatigue loading is still ongoing, from which a strain-based damage variable could be constructed, and its evolution studied. Following this, the evolution of the elasticity modulus of concrete (both tangent and secant modulus) should be analyzed. Eventually, a cyclic constitutive model will be proposed, considering flexural tensile fatigue damage. With the aid of standard finite element software, the fatigue behavior of structural components such as concrete bridge decks, could be practically predicted with relative ease.

At last, it should be pointed out that only the Chinese standard was used in this study. One might justify that concrete is an engineering product highly dependent on local raw materials, and concrete must be produced, tested, and evaluated strictly according to national standards. Differences in the technical rules exist between various national and international codes and standards. For example, while $\Phi 150 \text{ mm} \times 300 \text{ mm}$ cylinders are

adopted to obtain the axial compressive strength in CEB-FIP, 150 mm × 150 mm × 300 mm prisms are specified in the governing Chinese code [25,29]. It would be desirable to compare CEB-FIP, Eurocode, RILEM, ACI, and the Chinese codes and standards regarding the requirements for mix design, slump evaluation, fatigue test specimens, and recommended $S-N$ curves. Comparative studies, like the one in the literature [30], should be conducted through international cooperation. This effort could contribute to avoiding repetition and confusion within the academic community and encouraging the convergence and standardization of sustainable development.

4. Conclusions

Four-point bending fatigue tests of 55 plain concrete (PC series) and 42 reinforced concrete (RC series) beams were conducted for the flexural fatigue properties of normal-grade C50 ordinary concrete, and the fatigue life data of test specimens were analyzed and fitted to semi-logarithmic and logarithmic equations. Probabilistic fatigue equations with a failure probability p varying from 0.1 to 0.5 for specimens with a fixed minimum stress level of 0.10, and when considering a stress ratio R varying from about 0.11 to 0.44, were obtained respectively through regression analysis. These fatigue equations were then compared to those available in the literature. The following conclusions are drawn:

- (1) Two-parameter Weibull distribution could describe the fatigue life of specimens tested under the same maximum stress level S_{\max} . The semi-logarithmic and logarithmic equations were nearly identical at the tested stress levels, with the latter predicting longer fatigue life for $S_{\max} < 0.70$.
- (2) The stress ratio R is an essential factor affecting the fatigue life of concrete, the effect of which shall not be ignored and can be conveniently considered through the equivalent fatigue life $\bar{N} = N^{1-R}$.
- (3) Although the PC specimens failed in brittle fracture and the RC series exhibited ductile behavior after macroscopic concrete cracking appeared, the fatigue cracking life of these series are relatively close, with the latter slightly longer. The restraining effect from steel reinforcement influences the fatigue crack initiation of concrete.
- (4) Fatigue equations of normal-grade C50 ordinary concrete lie slightly below those of high-strength concrete. Although not as important as the maximum stress level and the stress ratio, the material strength grade affects ordinary concrete's flexural fatigue properties.
- (5) During the stress-controlled bending fatigue tests, the measured concrete strain developed in a three-stage manner with a continuously increasing value. The maximum longitudinal strain in the concrete just before fatigue failure was in reverse proportion to the maximum stress level applied.

In the future, the evolution of cyclic strain, the stiffness degradation, and the fatigue damage constitutive relationship shall be established to lay a foundation for the fatigue assessment of reinforced concrete structures.

Author Contributions: Conceptualization, H.C.; methodology, H.C. and J.F.; software, Z.S. and X.Z.; validation, H.C., Z.S. and J.F.; formal analysis, Z.S. and X.Z.; investigation, X.Z. and Z.S.; resources, H.C. and J.F.; data curation, Z.S. and X.Z.; writing—original draft preparation, X.Z. and H.C.; writing—review and editing, H.C., Z.S., X.Z. and J.F.; visualization, H.C. and Z.S.; supervision, H.C. and J.F.; project administration, H.C. and J.F.; funding acquisition, H.C. All authors have read and agreed to the published version of the manuscript.

Funding: This research was funded by the National Natural Science Foundation of China, grant number 52278137. The APC was funded by the open access program of Beijing University of Technology.

Institutional Review Board Statement: Not applicable.

Informed Consent Statement: Not applicable.

Data Availability Statement: Details of the experimental data presented in this study are available upon reasonable request to the corresponding author.

Conflicts of Interest: The authors declare no conflict of interest. The funders had no role in the design of the study; in the collection, analyses, or interpretation of data; in the writing of the manuscript; or in the decision to publish the results.

References

1. Chen, H.T.; Zhan, X.W.; Zhu, X.F.; Zhang, W.X. Fatigue evaluation of steel-concrete composite deck in steel truss bridge—A case study. *Front. Struct. Civ. Eng.* **2022**, *16*, 1336–1350. [[CrossRef](#)]
2. Chen, X.D.; Xu, L.Y.; Shi, D.D.; Chen, Y.Z.; Zhou, W.; Wang, Q. Experimental study on cyclic tensile behaviour of concrete under various strain rates. *Mag. Concr. Res.* **2018**, *70*, 55–70. [[CrossRef](#)]
3. Tepfers, R.; Kutti, T. Fatigue strength of plain, ordinary and lightweight concrete. *J. Proc.* **1979**, *76*, 635–652.
4. Oh, B.H. Fatigue analysis of plain concrete in flexure. *J. Struct. Eng.* **1986**, *112*, 273–288. [[CrossRef](#)]
5. Oh, B.H. Fatigue life distributions of concrete for various stress levels. *Mater. J.* **1991**, *88*, 122–128.
6. Kachkouch, F.Z.; Noberto, C.C.; Babadopulos, L.F.D.L.; Melo, A.R.S.; Machado, A.M.L.; Sebaibi, N.; Boukhelf, F.; El Mendili, Y. Fatigue behavior of concrete: A literature review on the main relevant parameters. *Constr. Build. Mater.* **2022**, *338*, 127510. [[CrossRef](#)]
7. Zhao, G.Y.; Wu, P.G.; Zhan, W.W. The fatigue behaviour of high-strength concrete under tension cyclic loading. *China Civ. Eng. J.* **1993**, *26*, 13–19.
8. Li, Y.Q.; Che, H.M. Study on fatigue of plain concrete under constant amplitude flexural cyclic loading. *J. China Railw. Soc.* **1999**, *2*, 76–79.
9. Shi, X.P.; Yao, Z.K.; Li, H.; Lin, T. Study on flexural fatigue behavior of cement concrete. *China Civ. Eng. J.* **1990**, *3*, 11–22.
10. Wu, Y.Q.; Gu, H.J.; Li, H.C. The S-P-N equation of concrete flexural tensile fatigue. *Concrete* **2005**, *36*, 46–48.
11. Mohammadi, Y.; Kaushik, S.K. Flexural fatigue-life distributions of plain and fibrous concrete at various stress levels. *J. Mater. Civ. Eng.* **2005**, *17*, 650–658. [[CrossRef](#)]
12. Stefanidou, M.; Kamperidou, V.; Konstantinidis, A.; Koltsou, P.; Papadopoulos, S. Rheological properties of biofibers in cementitious composite matrix. In *Advances in Bio-Based Fiber*; Rangappa, S.M., Puttegowda, M., Parameswaranpillai, J., Siengchin, S., Gorbatyuk, S., Eds.; Woodhead Publishing: Cambridge, UK, 2022; pp. 553–573.
13. Zheng, K.R.; Sun, W.; Miao, C.W.; Guo, L.P.; Zhou, W.L.; Chen, H.J. Effects of mineral admixtures on fatigue behavior of concrete. *J. Build. Mater.* **2007**, *4*, 379–385.
14. Soheli, K.M.A.; Al-Jabri, K.; Zhang, M.H.; Liew, J.Y.R. Flexural fatigue behavior of ultra-lightweight cement composite and high strength lightweight aggregate concrete. *Constr. Build. Mater.* **2018**, *173*, 90–100. [[CrossRef](#)]
15. Zhang, Y.Y.; Sun, Q.; Xin, H.H.; Liu, Y.Q.; Correia, J.A.F.O.; Berto, F. Probabilistic flexural fatigue strength of ultra-lightweight cement concrete and high strength lightweight aggregate concrete. *Int. J. Fatigue* **2022**, *158*, 106743. [[CrossRef](#)]
16. Saini, B.S.; Singh, S.P. Flexural fatigue strength prediction of self compacting concrete made with recycled concrete aggregates and blended cements. *Constr. Build. Mater.* **2020**, *264*, 120233. [[CrossRef](#)]
17. Saini, B.S.; Singh, S.P. Fatigue life prediction of self compacting concrete made with recycled concrete aggregates under flexural loading. *J. Sustain. Cen.-Based Mater.* **2020**, *11*, 1–20. [[CrossRef](#)]
18. Zhou, J.Z.; Fu, T.T.; Zhong, C.H.; Peng, K.; Shuang, Z.Y. Flexural fatigue behaviors of silicon carbide recycled concrete in corrosive environments. *Adv. Civ. Eng.* **2021**, *2021*, 7459777. [[CrossRef](#)]
19. Dong, S.F.; Wang, X.Y.; Ashour, A.; Han, B.G.; Ou, J.P. Enhancement and underlying mechanisms of stainless steel wires to fatigue properties of concrete under flexure. *Cem. Concr. Compos.* **2022**, *126*, 104372. [[CrossRef](#)]
20. Liu, F.P.; Zhou, J.T. Concrete bending strength degradation analysis based on fatigue strain evolution. *China J. Highw. Transp.* **2017**, *30*, 97–105.
21. Zhao, D.F.; Gao, H.J.; Yang, J.H. Variable-amplitude fatigue properties of plain concrete under biaxial tension-compression and triaxial tension-compression-compression cyclic loading. *Eng. Mech.* **2017**, *34*, 154–160.
22. Wei, J.; Li, S.L.; Dong, R.Z.; Liu, X.C.; Wu, Z.Q. Fatigue damage constitutive model of concrete considering the effect of residual deformation. *J. Hunan Univ.* **2016**, *43*, 57–61.
23. Oneschkow, N. Fatigue behaviour of high-strength concrete with respect to strain and stiffness. *Int. J. Fatigue* **2016**, *87*, 38–49. [[CrossRef](#)]
24. Chen, B.; Wang, J. Flexural fatigue life reliability of alkali-activated slag concrete freeze-thaw damage in cold areas. *Adv. Mater. Sci. Eng.* **2021**, *2021*, 1257163. [[CrossRef](#)]
25. GB/T 50081; Standard for Test Methods of Concrete Physical and Mechanical Properties. China Architecture & Building Press: Beijing, China, 2019; pp. 28–30.
26. Ou, J.P.; Lin, Y.Q. Experimental study on performance degradation of plain concrete due to high-cycle fatigue damage. *China Civ. Eng. J.* **1999**, *5*, 15–22.
27. Saini, B.S.; Singh, S.P. Flexure fatigue strength and failure probability of self compacting concrete made with RCA and blended cements. *Structures* **2022**, *45*, 299–314. [[CrossRef](#)]

28. Chen, H.T.; Sun, Z.Y.; Zhong, Z.F.; Huang, Y. Fatigue factor assessment and life prediction of concrete based on Bayesian regularized BP neural network. *Materials* **2022**, *15*, 4491. [[CrossRef](#)]
29. CEB-FIP. *fib Model Code for Concrete Structures 2010*; Wilhelm Ernst & Sohn: Berlin, Germany, 2013.
30. Shi, J.H.; Wei, L.W.; Faidy, C.; Wasylyk, A.; Prinja, N. A Comparison of Different Design Codes on Fatigue Life Assessment Methods. In Proceedings of the ASME Pressure Vessels & Piping Division Conference, Vancouver, BC, Canada, 17–21 July 2016.

Disclaimer/Publisher's Note: The statements, opinions and data contained in all publications are solely those of the individual author(s) and contributor(s) and not of MDPI and/or the editor(s). MDPI and/or the editor(s) disclaim responsibility for any injury to people or property resulting from any ideas, methods, instructions or products referred to in the content.